pharmaceuticals

MDPI

Article

New N-Alkylated Heterocyclic Compounds as Prospective NDM1 Inhibitors: Investigation of In Vitro and In Silico Properties

Yassine Kaddouri [1,*,†], Btissam Bouchal [2], Farid Abrigach [3], Mohamed El Kodadi [3,4], Mohammed Bellaoui [2], Ahmed Elkamhawy [5,6], Rachid Touzani [3] and Magda H. Abdellattif [7,*,†]

1 Laboratory of Inorganic Chemistry, Department of Chemistry, University of Helsinki, P.O. Box 55, FI-00014 Helsinki, Finland
2 Genetics Unit, Medical Sciences Research Laboratory, Faculty of Medicine and Pharmacy of Oujda, University Mohammed Premier, Oujda 11022, Morocco; btissam.bouchal@gmail.com (B.B.); bmbellaoui@gmail.com (M.B.)
3 Laboratory of Applied Chemistry & Environment (LCAE), Faculty of Sciences, University Mohammed Premier, Oujda 11022, Morocco; f.abrigach@ump.ac.ma (F.A.); elkodadim@gmail.com (M.E.K.); r.touzani@ump.ac.ma (R.T.)
4 CRMEF Oriental, Center régional des Métiers de l'Education et de Formation, Oujda 11022, Morocco
5 BK21 FOUR Team and Integrated Research Institute for Drug Development, College of Pharmacy, Dongguk University-Seoul, Goyang 10326, Korea; a_elkamhawy@mans.edu.eg
6 Department of Pharmaceutical Organic Chemistry, Faculty of Pharmacy, Mansoura University, Mansoura 35516, Egypt
7 Chemistry Department, Sciences College, Taif University, P.O. Box 11099, Taif 21944, Saudi Arabia
* Correspondence: yassine.kaddouri92@gmail.com (Y.K.); m.hasan@tu.edu.sa (M.H.A.)
† These authors contributed equally to this work.

check for updates

Citation: Kaddouri, Y.; Bouchal, B.; Abrigach, F.; El Kodadi, M.; Bellaoui, M.; Elkamhawy, A.; Touzani, R.; Abdellattif, M.H. New N-Alkylated Heterocyclic Compounds as Prospective NDM1 Inhibitors: Investigation of In Vitro and In Silico Properties. *Pharmaceuticals* **2022**, *15*, 803. https://doi.org/10.3390/ph15070803

Academic Editors: Mary J. Meegan and Daniela Catarzi

Received: 18 February 2022
Accepted: 21 June 2022
Published: 28 June 2022

Publisher's Note: MDPI stays neutral with regard to jurisdictional claims in published maps and institutional affiliations.

Abstract: A new family of pyrazole-based compounds (**1**–**15**) was synthesized and characterized using different physicochemical analyses, such as FTIR, UV-Visible, ^{1}H, ^{13}C NMR, and ESI/LC-MS. The compounds were evaluated for their in vitro antifungal and antibacterial activities against several fungal and bacterial strains. The results indicate that some compounds showed excellent antibacterial activity against *E. coli*, *S. aureus*, *C. freundii*, and *L. monocytogenes* strains. In contrast, none of the compounds had antifungal activity. Molecular electrostatic potential (MEP) map analyses and inductive and mesomeric effect studies were performed to study the relationship between the chemical structure of our compounds and the biological activity. In addition, molecular docking and virtual screening studies were carried out to rationalize the antibacterial findings to characterize the modes of binding of the most active compounds to the active pockets of NDM1 proteins.

Keywords: synthesis; pyrazole; antibacterial; antifungal; ADME-Tox; molecular docking

1. Introduction

Resistance to antibiotics pushes researchers to discover new antibacterial candidates as prospective treatments for different infectious diseases with another class of antibiotics with specific mechanisms of action.

Beta-lactam antibiotics [1,2], commonly known as penicillin-binding proteins (PBPs), act as mechanism-based inhibitors by targeting the cell wall-modifying DD-transpeptidases, susceptible to nucleophilic attack from long-lived acylated complexes. PBPs are responsible for the formation and integrity of the membrane surface's rigid mesh-like peptidoglycan layer exterior. However, there is a mechanism of resistance to beta-lactam due to beta-lactamases. Where Ampicillin was selected as an example for this study, the selection was because it has an amine and carbonyl function similar to our first target compound (Figure 1) that binds to the penicillin-binding proteins. Commonly used broad-spectrum antibiotics are streptomycin [3–9] and cefotaxime [10,11], a third-generation cephalosporin [5,12–14] with less susceptibility to beta-lactamase [15–17] than ampicillin [5,18–20].

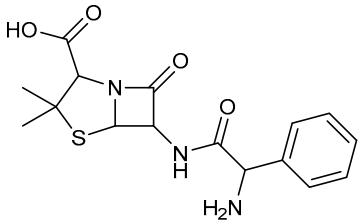

Figure 1. Chemical structure of Ampicillin.

Infectious diseases are the main threat, especially in developing countries [21], and include listeriosis [4,22–24] caused by *L. monocytogenes*, septicemia, and meningitis caused by *E. coli* [8,25], bloodstream infections, and meninges caused by *C. freundii* [26–29]. These diseases commonly affect healthy, sensitive individuals, such as older people, pregnant women, and the immunosuppressed [11]. In addition, however, candidiasis and related fungal bloodstream infections are caused by *Saccharomyces cerevisiae* [30], *Candida albicans*, and *Candida glabrata* [31].

Pyrazole-based heterocyclic ligands have multiple biological applications. Many compounds prepared in our research group already have high efficiencies [32–43] as antibacterial or antifungal candidates [34,38,44–46] due to their nitrogen electron and proton acceptor abilities [32]. With limited facilities to investigate more experimental properties, molecular docking [43,47–57] becomes crucial for studying the binding modes and affinities between the prepared compounds and selected biological targets using the lock and key concept. In our study, various tripodal pyrazole ligands were prepared and characterized using FTIR, UV-visible, ^{1}H, and ^{13}C NMR, and then their toxicity predictions and the Lipinski rule of five agreement were determined. Finally, the molecular ligand-protein docking, through the New Delhi metallo β-lactamase hydrolysis of β-lactams antibiotics [17,54,58,59], was studied in two different active sites to investigate our studied compounds' binding susceptibility to the hydrolase enzyme.

2. Results and Discussion

2.1. Antibacterial and Antifungal Activities

The antibacterial potential of the compounds against two Gram-negative bacterial strains (*Escherichia coli* and *Citrobacter freundii*) and two Gram-positive bacteria (*Staphylococcus aureus* and *Listeria monocytogenes*) was evaluated as described in the materials and methods section, and the results are displayed in Table 1. Only compounds **12** and **14** showed antibacterial activity when tested at 500 µM. Compound **12** was active against *E. coli*, *S. aureus,* and *C. freundii* but inactive against *L. monocytogenes,* whereas compound **14** was only active against *L. monocytogenes*.

Table 1. The antibiotic activity of the active synthesized pyrazole ligands was determined using the broth macro dilution assay and the phenol red indicator.

Compound	*L. monocytogenes*	*S. aureus*	*E. coli*	*C. freundii*
12	− − −	+ + +	+ + +	+ + +
14	+ + +	− − −	− − −	− − −
Streptomycin	+ + +	+ + +	+ + +	+ + +

The compounds and the positive control (streptomycin) were used at 500 µM and 50 mg/L concentrations. All experiments were repeated three times, and the result obtained for each time is presented. (−): no inhibition of bacterial growth; (+): inhibition of bacterial growth.

The MICs of compounds **12** and **14** were then determined as described in the material and methods (Table 2). The MIC of compound **12** was 134.9 mg/L against *E. coli*, 168.7 mg/L against *S. aureus*, and 168.7 mg/L against *C. freundii.* For compound **14**, the MIC against *L. monocytogenes* was 134.6 mg/L. Interestingly, the determination of the MBC

of these compounds showed that they are bactericidal, as demonstrated by the ratio of MBC/MIC ≤ 2 (Table 2).

Table 2. MIC and MBC values in mg/L of the studied compounds **12** and **14** against the used bacterial strains.

		12	**14**
L. monocytogenes	**MIC**	-	134.6 ± 0
	MBC	-	242.3 ± 0
	MBC/MIC	-	1.2
S. aureus	**MIC**	168.7 ± 0	-
	MBC	202.4 ± 0	-
	MBC/MIC	1.2	-
E. coli	**MIC**	134.9 ± 0	-
	MBC	134.9 ± 0	-
	MBC/MIC	1	-
C. freundii	**MIC**	168.7 ± 0	-
	MBC	236.2 ± 0	-
	MBC/MIC	1.4	-

MIC: Minimum inhibition concentration; **MBC:** Minimum bactericidal concentration.

Regarding the antifungal activity, all the compounds were tested for toxicity against *Saccharomyces cerevisiae* and two species of Candida, *Candida glabrata* and *Candida albicans*, as described in Section 3.3.3. All compounds showed no antifungal activity against all three strains used. Together with the antibacterial activity analysis, these results suggest that compounds **1** to **15** lack antifungal activity, and only compounds **12** and **14** act specifically as antibacterial agents.

*2.2. MEP Analysis of the Compounds **12**, **14**, Ampicillin, and Cefotaxime*

Molecular electrostatic potential (MEP) maps of compounds **12**, **14**, Ampicillin, and cefotaxime have been generated (Figure 2) to determine and predict the reactive sites (nucleophilic or electrophilic) on the molecular system of the studied compounds.

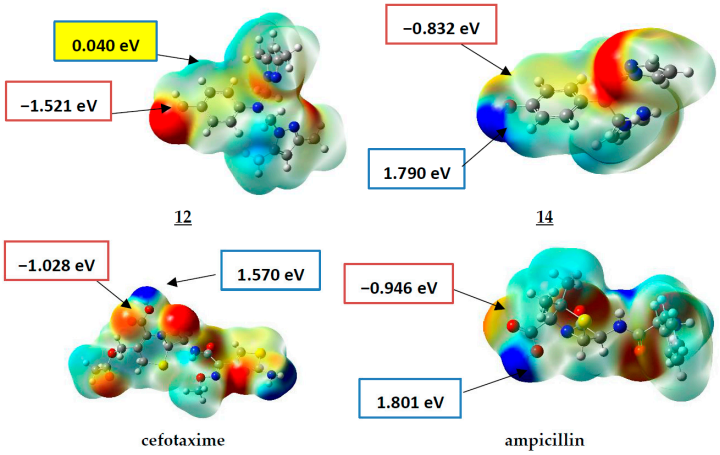

Figure 2. MEP surfaces of compounds **12**, **14**, ampicillin, and cefotaxime (-4.300×10^{-3} (Red) to 4.300×10^{-3} (Blue)).

As presented in Figure 2, the positive electrostatic potential areas (in blue) are concentrated over the hydroxyl group of the drugs cefotaxime and Ampicillin with 1.570 and 1.801 eV (at an iso value of 0.0004 electrons/Å^3). For compound **14**, the highest value was about 1.790 eV (located on the hydroxyl group substituent on the phenyl ring), while a low value of 0.040 eV was estimated for compound **12**.

The negative electrostatic potential areas are located over the carbonyl group of the acidic function of the drugs cefotaxime and Ampicillin, with values of −1.028 and −0.946 eV, respectively, with a higher value for the compound **12,** with the value of −1.521 eV. In comparison, it was −0.832 eV for compound **14**.

To sum up, compound **12** only has a higher negative charge value over the carbonyl. In contrast, compound 14, similar to the antibiotics cefotaxime and Ampicillin, has lower negative–positive (δ^+-δ^-) charge values over the hydroxyl and the acidic function. These results, which agree with the experimental results, give us information about the possible sites for binding modes to the biological targets that need molecular docking investigations.

In general, and in the light of these observations, we can postulate that the substitution by groups with different electronic effects (withdrawing-donating) is more beneficial in improving the antibacterial potency than the substitution by one group (Figure 3).

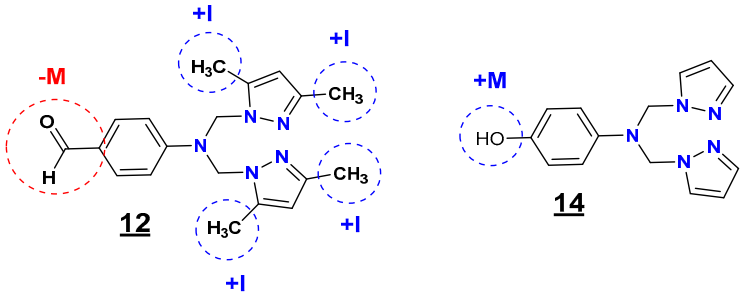

Figure 3. Inductive and mesomeric effect study of the compounds **12** and **14**.

Regarding the R_1 (substituent on the phenyl ring) and R_2 (substituent at positions 3 and 5 of the pyrazole moiety) substituents, the inductive and mesomeric effect study revealed that the presence of the formyl (CHO) group (electron-withdrawing effect (-M)) on the phenyl ring and the methyl (CH_3) groups (electron-donating effect (+I)) on the pyrazole moieties at positions 3 and 5 (**12**) is highly favorable for the inhibitory potency against *E. coli*, *S. aureus*, and *C. freundii* strains. In contrast, the presence of the hydroxyl (OH) group (electron-donating effect (+M)) on the phenyl ring with non-substituted pyrazole moieties (**14**) resulted in selective antibacterial activity against *L. monocytogenes*.

2.3. ADME and Toxicity Predictions

ADME Predictions

For the ADME predictions, the physicochemical properties (MW: molecular weight expressed in Daltons; logP: octanol/water partition coefficient characterizing Lipophilicity; HDO: number of hydrogen bond donors; HAC: number of hydrogen bond acceptors; NRO: number of rotatable bonds; TPSA: total polar surface area) were calculated and are presented in Table 3 for the compounds **12** and **14** and the drugs streptomycin, Ampicillin, and cefotaxime as references.

Table 3. The physicochemical properties of the compounds **12**, **14,** and the drugs streptomycin, Ampicillin, and cefotaxime.

Compound	MW	logP	HDO	HAC	NRO	TPSA (Å^2)
12	337.42	3.09	0	3	6	55.95
14	269.30	1.22	1	3	5	59.11
streptomycin	581.57	−6.65	14	15	11	331.43
ampicillin	349.40	0.26	3	5	5	138.03
cefotaxime	455.47	−0.73	3	9	9	227.05

In Table 4, compounds **12** and **14** have no violations of Lipinski's rule of five [58,59], with MW = 337.42 and 269.30 < 500, logP value of 3.0933 and 1.227 < 5, H donor of 0 and 1 < 5, H acceptor of 3 and 3 < 10, number of rotatable bonds of 6 and 5 < 10 and TPSA value

of 55.95 and 59.11 Å^2 < 140 Å^2. This comparison highlights that the two compounds **12** and **14** have better oral bioavailability than Ampicillin and are better than streptomycin.

Table 4. The binding affinity values of the compounds **12**, **14**, and ampicillin within the two NDM1 chains A and B.

Compound	NDM1 (A) Binding Affinity in kcal/mol	NDM1 (B) Binding Affinity in kcal/mol
12	−6.0075	−6.6776
14	−5.5411	−5.6752
ampicillin	−6.9737	−6.7344

These results make compound **12** a better antibacterial candidate than cefotaxime with the same selective multitarget activity, but further toxicity predictions are required to validate these propositions.

2.4. Molecular Docking and Virtual Screening Studies

Ligand–protein docking simulations were carried out to determine the binding mode of the studied compounds with the catalytic sites of the selected receptors. Flexibility was allowed in all the rotatable bonds of the ligand; the protein was used as a rigid structure.

2.4.1. Docking against the NDM-1 β-lactamase (NDM1) Protein

NDM-1 β-lactamase hydrolysis docking study of the compounds **12** and **14** compared to Ampicillin.

The three-dimensional structure of New Delhi metallo-β-lactamase (NDM1) [17,58,59] is represented in Figure 4, where two sequences, A and B, were co-crystalized with Ampicillin; so in this part, we studied the binding affinity of the compounds **12** and **14** compared to Ampicillin.

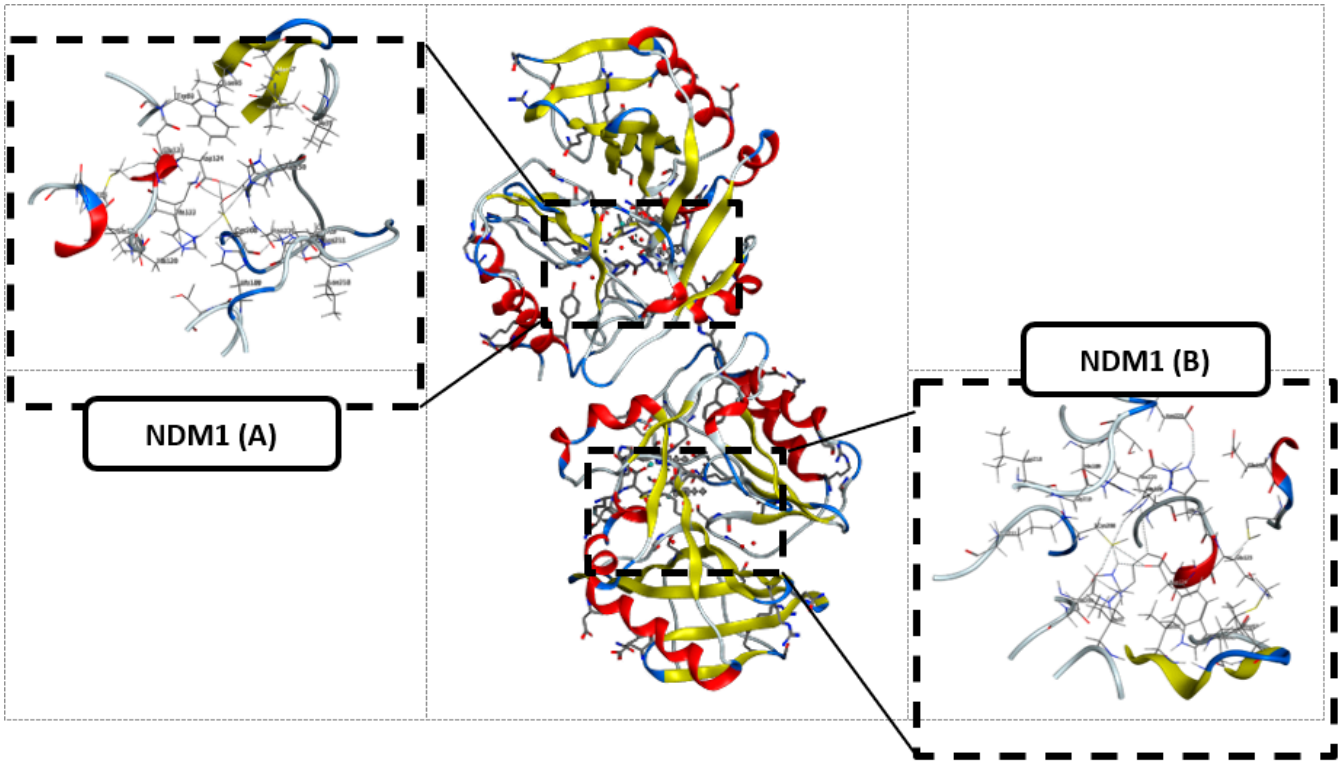

Figure 4. The three-dimensional structure of New Delhi metallo-β-lactamase (NDM1) and the two selected active sites.

The protein preparation was performed by removing all the water, zinc, and OH molecules.

As previously mentioned in the docking study of the transpeptidase inhibition study, the NDM1 hydrolysis followed the same parameters, and the binding affinity results of both active sites are collected in Table 4.

From Table 5, compound **12** had a better affinity than compound **14** in both selected active sites, NDM1 A and B, with a binding affinity of −6.0075 and −6.6776 Kcal/mol, respectively. In addition, compared to Ampicillin, with −6.9737 and −6.7344 Kcal/mol, compound **12** was more readily hydrolyzed than compound **14**.

Table 5. Docking results of the compounds **12**, **14**, and ampicillin in the two NDM1 chains A and B.

	NDM1 (A)		NDM1 (B)	
Compound	**Interaction L-AA**	**Bond Length (Å)**	**Interaction L-AA**	**Bond Length (Å)**
12	O47—ND1 His 122: **H-acceptor**	3.08	O47—NZ Lys211: **H-acceptor**	2.98
	O47—NE2 His 189: **H-acceptor**	2.9	5-ring—r-ring His 122: **pi-pi**	3.62
14	6-ring—N Asn 220: **pi-H**	3.9	6-ring—N Asn220: **pi-H**	3.89
	5-ring—5-ring His 122: **pi-pi**	3.6	5-ring—5-ring His 122: **pi-pi**	3.64
ampicillin	OXT45—OD1 Asp124: **H-donor**	2.9		
	O1 1—NZ Lys211: **H-acceptor**	3.37		
	O2 3—NZ Lys211: **H-acceptor**	2.98	OXT45—OD1 Asp124: **H-donor**	2.99
	O3 28—N Asp124: **H-acceptor**	3.55	O1 1—NZ Lys211: **H-acceptor**	2.88
	C16 12—5-ring His 250: **H-pi**	4.07	O3 28—N Asp124: **H-acceptor**	3.38
	6-ring—N Gln 123: **pi-H**	4.08		
	6-ring—CB Gln 123: **pi-H**	3.78		

First, compound **12** has two H-acceptors, bond 3.08 and 2.90 Å, respectively, between the carbonyl and the nitrogen ND1 and NE2 of His122 and His 189, as shown in Table 5 and Figure 5.

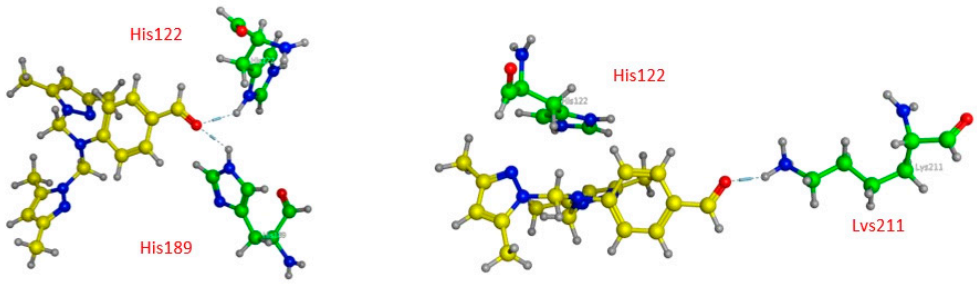

Figure 5. Three-dimensional presentations of the binding modes between the compound **12** and NDM1.

Contrary to compound **12**, compound **14**, as represented in Figure 6, has only weak van der Waals bonds with Asn 220 and His 122, with a distance range of 3.60–3.90 Å, making this compound more stable against NDM1 hydrolysis.

As penicillin β-lactam antibiotics reported in the literature, Ampicillin seems to interact with more residues at the site (A) than at the site (B) of NDM1 protein, as represented in Table 5 and Figure 7. In the active pocket A, the compound forms seven bonds: one H-donor and one H-acceptor (of 2.90 and 3.55 Å, respectively) with Asp124 residue, two H-acceptor bonds with Lys211 amino acid with distances equal to 2.98 and 3.37 Å, one H-pi interaction (4.07 Å) between the carbon (C16 12) atom and 5-ring of His250, and two pi-H interactions between the 6-ring and the nitrogen and carbon atoms of Gln123 (4.08 and 3.78 Å). In contrast, Ampicillin was found to bind into the active pocket B of NDM1 only with three interactions: two by H-donor and H-acceptor bonds with Asp124 (2.99 and 3.55 Å) and one by an H-acceptor bond with Lys211 with a distance of 2.88 Å involving its oxygen atom (O1 1).

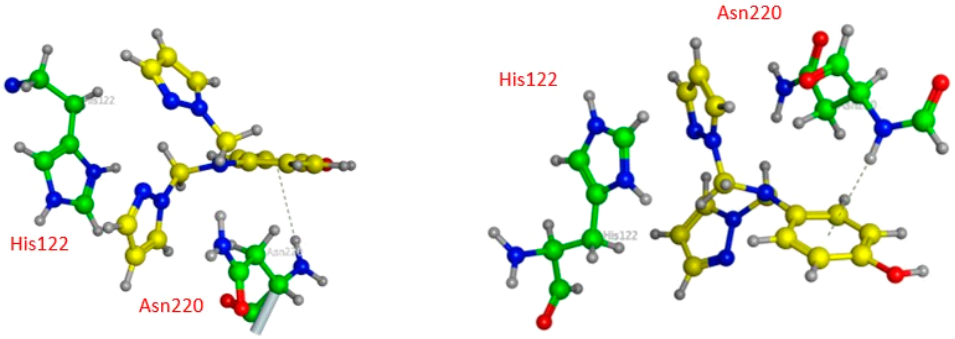

Figure 6. Three-dimensional presentations of the binding modes between the compound **14** and NDM1.

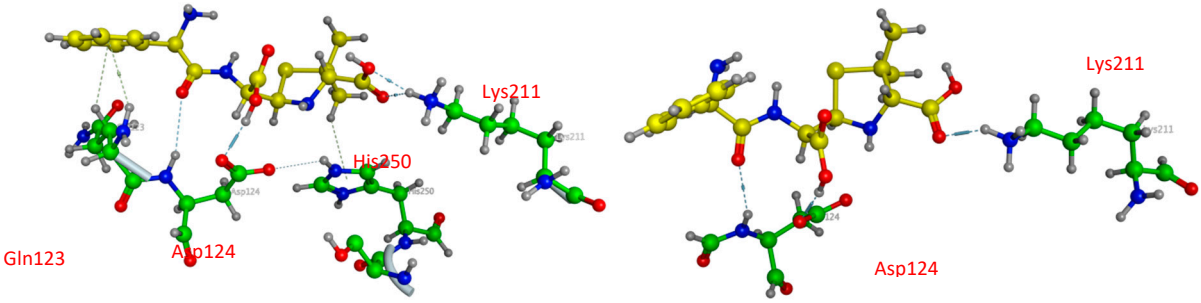

Figure 7. Three-dimensional presentations of the binding modes between Ampicillin and NDM1.

From the docking study results, compound **12** is more sensitive to NDM1 hydrolysis, which inactivates its antibacterial activity against *Listeria monocytogenes* due to the common carbonyl function in all β-lactam antibiotics. Although otherwise, compound **14** has listericidal activity due to its weak binding with the selected NDM1, its specific mechanism needs more computational studies and biological assays for prediction.

2.4.2. Blind Docking/Virtual Screening against the NDM-1 β-lactamase (NDM1) Protein

As presented in Figure 8, the B-chain has considered the active site with all the docking poses. At the same time, there is good alignment between the ligand **12** and ampicillin docking poses with smooth variation, while ligand **14** is so far in a different site.

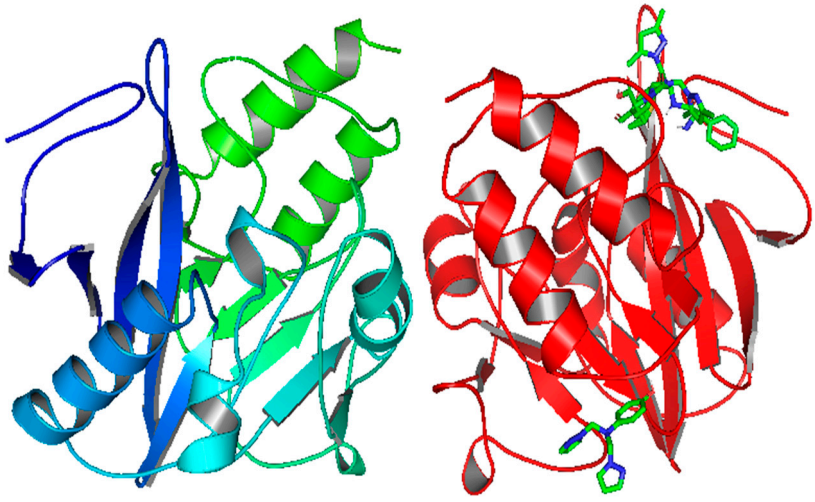

Figure 8. Docking poses of the ligands **12**, **14,** and **ampicillin** in the NDM1 protein (PDB: 5ZGE).

Table 6 shows that the mode of binding interaction is the same as that of LYS216, which is bound with the nitrogen of pyrazole for the ligand **12** and the oxygen for Ampicillin with the same binding affinity of −7.1 Kcal/mol. On the other hand, ligand **14** has a lower −7.0 Kcal/mol value with amino acids such as ILE203 and LYS242.

Table 6. Binding affinity and L–AA interaction of the ligands **12** and **14** and ampicillin with the chosen target, NDM1.

Compound	Binding Affinity in kcal/mol	Interaction L–AA (Hydrogen Bonds Only)
12	−7.1	N(pyrazole)—LYS216
14	−7.0	OH—-ILE203 N(pyrazole)—LYS242
ampicillin	−7.1	NH2—SER251 NH2—HIS250 O—LYS216

3. Materials and Methods

3.1. Analytical Procedures

A Bruker DPX 800 MHz Spectrometer recorded the ^{1}HNMR (500 MHz, DMSO-*d*6) and ^{13}CNMR (125 MHz, chloroform-*d)* spectra. Chemical shift (δ) values were stated in parts per million (ppm) using internal standard tetramethylsilane, according to the D_2O exchange. Chemical shift (d) values were stated in parts per million (ppm) using internal standard tetramethylsilane. The D_2O exchange confirmed the exchangeable protons (OH and NH). The FTIR analyses were performed using an FTIR 8400S spectrophotometer recorded in KBr pellets.

Many different pyrazole derivatives were synthesized and indexed.

3.2. Chemistry

The pyrazole derivatives (Figure 9) investigated in this work were prepared following the experimental procedure of the *N*-alkylation reaction described previously in the literature [43,46,60–77]. First, all the compounds were prepared by condensation of primary amines with (3,5-dimethyl-*1H*-pyrazole-1-yl)methanol or (*1H*-pyrazole-1-yl)methanol in acetonitrile as a polar aprotic solvent that promotes SN2 reaction; after that, the compounds were purified either by diethyl ether or a DCM:water (3:1) mixture to obtain the final products, with yields varying from 15.22 to 99.41%.

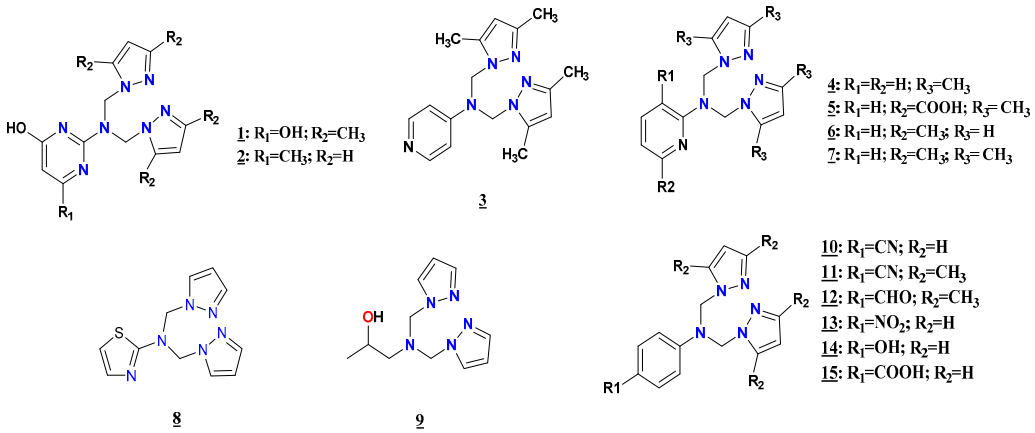

Figure 9. Structures of the compounds **1**–**15**.

2-(Bis((3,5-dimethyl-*1H*-pyrazol-1-yl)methyl)amino)pyrimidine-4,6-diol (**1**)

2-Aminopyrimidine-4,6-diol (1 g, 7.86 mmol) and (3,5-dimethyl-*1H*-pyrazol-1-yl)methanol (1.98 g, 15.72 mmol) were mixed together in acetonitrile (20 mL) under reflux for 4 h, and the

solvent was evaporated, then recrystallized in diethyl ether, and then filtrated to obtain the final product (1.28 g, 47.4%), mp > 250 °C (diethyl ether); FTIR (KBr, cm^{-1}): 3348 (-OH); 3149 (C-H); 1684 (C=C); 1560 (C-C); 1455 (C-N); 1266 (C=N); 1067 (N-N); 779 (=C-H); ^{1}H NMR (DMSO-d_6, 500 MHz) δ ppm: 6.47 (s, 4H, H-CH_2); 5.76 (s, 4H, H-OH and Hpyrz-4)); 5.25 (s, 1H, Hpyrm); 2.14 (s, 12H, Hpyrz), ^{13}C NMR (DMSO-d_6, 125 MHz) δ ppm: 105.46 (Cpyrz); 70.38 (CH_2); 10.75 (Cpyrz-5); 10.19 (Cpyrz-3). The elemental Analysis was calculated for $C_{16}H_{21}N_7O_2$ (M.wt 384.13); C-55.96; H-6.16; and N-28.55 were the % calculated. C-55.81; H-6.06; and N-28.55 were the % found.

2-(Bis((*1H*-pyrazol-1-yl)methyl)amino)-6-methylpyrimidin-4-ol (**2**)

2-Amino-6-methylpyrimidine-4-ol (1 g, 7.99 mmol) and (*1H*-pyrazol-1-yl)methanol (1.57 g, 15.98 mmol) were mixed together in acetonitrile (20 mL) under reflux for 4 h, and the solvent was evaporated, then recrystallized in diethyl ether, and then filtrated to obtain the final product (3.8 g, 91.22%): mp > 250 °C (diethyl ether); FTIR (KBr, cm^{-1}): 3328 et 3069 (O-H Free and linked); 2925 (C-H); 1656 (C=C); 1493 (C-C); 1383 (C-N); 1172 (C=N); 1049 (N-N); 763 (=C-H); ^{1}H NMR (DMSO-d_6, 400 MHz) δ ppm: 10.53 (s, 1H, H-OH); 7.61 (d, 2H, Hpyrz-5, J_{H-H} = 4–6 Hz); 7.30 (d, 2H, Hpyrz-3, J_{H-H} = 4–6 Hz); 6.10 (m, Hpyrm-4); 4.82 (s, H-CH_2 and Hpyrm); 1.91 (s, CH_3); ^{13}C NMR (DMSO-d_6, 100 MHz) δ ppm: 137.65 (Cpyrz-3); 128.99 (Cpyrz-5); 104.67 (Cpyrz-4); 104.59 (Cpyrm); 73.69 (CH_2); 21.59 (CH_3).).The elemental Analysis was calculated for $C_9H_9N_3O_4S$ (M.wt 255); C-54.73; H-5.30; and N-34.37 were the % calculated. C-54.65; H-5.21; N-34.29 were the % found.

N,N-bis((3,5-dimethyl-*1H*-pyrazol-1-yl)methyl)pyridin-4-amine (**3**) [61]

4-Aminopyridine (0.5 g, 5.31 mmol) and (3,5-dimethyl-*1H*-pyrazol-1-yl)methanol (1.34 g, 10.62 mmol) were mixed together in acetonitrile (20 mL) under reflux for 4 h, and the solvent was evaporated, then recrystallized in diethyl ether, and then filtrated to obtain the final product (0.48 g, 29.04%): mp 100–102 °C (diethyl ether); FTIR (KBr, cm^{-1}): 2359 (C-H); 1648 (C=C); 1559 (C-C); 1454 (C-N); 1310 (C=N); 1071 (N-N); 807 (=C-H); ^{1}H NMR ($CDCl_3$, 500 MHz) δ ppm: 7.66 (d, 1H, Hpyrn-3, J_{H-H} = 5–6 Hz); 7.24 (d, 1H, Hpyrn-2, J_{H-H} = 5–6 Hz); 6.24 (s, 1H, Hpyrz-4); 5.66 (s, 2H, H-CH_2); 2.34 (s, 3H, $CH_3$$^{-}$5); 2.09 (s, 3H, CH_3-3); ^{13}C NMR ($CDCl_3$, 125 MHz) δ ppm: 167.73 (Cpyrn-1); 156.11 (Cpyrn-2); 140.41 (Cpyrz-3); 138.13 (Cpyrz-5); 113.78 (Cpyrn-3); 105.50 (Cpyrz-4); 57.61 (2H, CH_2); 14.02 (Cpyrz-3); 10.96 (Cpyrz-5).

N,N-bis((3,5-dimethyl-*1H*-pyrazol-1-yl)methyl)pyridin-2-amine (**4**) [78,79]

2-Aminopyridine (0.5 g, 5.31 mmol) and (3,5-dimethyl-*1H*-pyrazol-1-yl)methanol (1.34 g, 10.62 mmol) were mixed together in acetonitrile (20 mL) at room temperature for 4 days, and the solvent was evaporated, then recrystallized in diethyl ether, and then filtered to obtain the final product (1.51 g, 92.13%): mp 88–90 °C (diethyl ether); FTIR (KBr, cm^{-1}): 1609 (C=C); 1530 (C-C); 1423 (C-N); 1291 (C=N); 1067 (N-N); 772 (=C-H); ^{1}H NMR ($CDCl_3$, 500 MHz) δ ppm: 8.01 (d, 1H, Hpyrn-3, J_{H-H} = 5–6 Hz); 7.31 (d, 1H, Hpyrn-4, J_{H-H} = 4–6 Hz); 6.54 (dd, 1H, Hpyrn-5, J_{H-H} = 4–6 Hz and J_{H-H} = 5–6 Hz); 6.45 (d, 1H, Hpyrn-2, J_{H-H} = 4–6 Hz); 6.38 (d, Hpyrn-6, J_{H-H} = 5–6 Hz); 5.67 (s, 1H, Hpyrz-4); 5.50 (s, 2H, CH_2); 2.35 (s, 3H, CH_3-5); 2.27 (s, 3H, CH_3-3); ^{13}C NMR ($CDCl_3$, 125 MHz) δ ppm: 156.65 (Cpyrn-1); 148.42 (Cpyrn-2); 147.41 (Cpyrz-3); 139.81 (Cpyrz-5); 137.49 (Cpyrn-4); 114.17 (Cpyrn-3); 109.03 (Cpyrn-2); 106.16 (Cpyrz-4); 54.33 (2H, CH_2); 13.43 (Cpyrz-3); 11.12 (Cpyrz-5).

2-(Bis((3,5-dimethyl-*1H*-pyrazol-1-yl)methyl)amino) nicotinic acid (**5**)

3-Amino-4-methylnicotinic acid (1 g, 7.24 mmol) and (3,5-dimethyl-*1H*-pyrazol-1-yl)methanol (1.82 g, 14.48 mmol) were mixed together in acetonitrile (20 mL) under reflux for 4 h, and the solvent was evaporated, then recrystallized in diethyl ether, and then filtrated to obtain the final product (0.37 g, 52.1%): mp 78–80 °C (diethyl ether); ^{1}H NMR (DMSO-d_6, 400 MHz) δ ppm: 7.87 (s, 2H, Hpyrn-4 and 6); 6.69 (s, 5H, Hpyrn-5, 2 CH_2); 5.37 (s, 2H, Hpyrz-4); 2.12 (s, 12H, Hpyrz-3, 5); ^{13}C NMR (DMSO-d_6, 100 MHz) δ ppm: 164.32 (COOH); 163.09 (Cpyrn-1); 154.75 (Cpyrn-4, Cpyrz-3); 110.89 (Cpyrn-5, COOH, Cpyrz-4); 54.24 (2 CH_2); 20.67 (4 CH_3). The elemental Analysis was calculated for $C_{18}H_{22}N_6O_2$

(M.wt 354.43); C- C-61.00, H-6.26, and N-23.71 were the % calculated. C-61.00; H-6.26; and N-23.71 were the % found.

N,N-bis((*1H*-pyrazol-1-yl)methyl)-6-methylpyridin-2-amine (**6**) [61]

2-Amino-6-methylpyrimidine (0.5 g, 4.75 mmol) and (*1H*-pyrazol-1-yl)methanol (0.93 g, 9.51 mmol) were mixed together in acetonitrile (20 mL) at room temperature for 4 days, and the solvent was evaporated, then recrystallized in diethyl ether, and then filtrated to obtain the final product (0.19 g, 15.22%): mp 78–80 °C (diethyl ether); FTIR (KBr, cm^{-1}): 3300 (N-H); 1614 (C=C); 1532 (C-C); 1473 (C-N); 1281 (C=N); 1082 (N-N); 747 (=C-H); ^{1}H NMR ($CDCl_3$, 500 MHz) δ ppm: 7.66 (d, 2H, Hpyrz-5, J_{H-H} = 4–6 Hz); 7.42 (d, 2H, Hpyrz-3, J_{H-H} = 5–6 Hz); 7.19 (dd, 1H, Hpyrn-2, J_{H-H} = 6–8 Hz and J_{H-H} = 8–10 Hz); 6.45 (d, 1H, Hpyrn-3, J_{H-H} = 4–6 Hz); 6.24 (dd, 2H, Hpyrz-4, J_{H-H} = 4–6 Hz and J_{H-H} = 5–6 Hz); 2.33 (s, 3H, Hpyrn-CH_3); 6.13 (d, 1H, Hpyrn-6, J_{H-H} = 4–6 Hz); 5.63 (s, 2H, H-CH_2); ^{13}C NMR ($CDCl_3$, 125 MHz) δ ppm: 156.49 (Cpyrz-5); 156.09 (Cpyrn-3); 132.46 (Cpyrn-6); 73.79 (Cpyrz-4); 59 (CH_2); 57.8 (Cpyrn-2); 23.76 (Cpyrn-CH_3).

N,N-bis((3,5-dimethyl-*1H*-pyrazol-1-yl)methyl)-6-methylpyridin-2-amine (**7**) [61]

2-Amino-6-methylpyridine (0.5 g, 4.62 mmol) and (3,5-dimethyl-*1H*-pyrazol-1-yl)methanol (1.17 g, 9.24 mmol) were mixed together in acetonitrile (20 mL) at room temperature for 4 days, and the solvent was evaporated, then recrystallized in diethyl ether, and then filtrated to obtain the final product (1.03 g, 68.7%): mp 96–98 °C (diethyl ether); FTIR (KBr, cm^{-1}): 3288 (N-H); 1612 (C=C); 1537 (C-C); 1433 (C-N); 1336 (C=N); 1072 (N-N); 774 (=C-H); ^{1}H NMR (CD_2Cl_2, 500 MHz) δ ppm: 7.33 (dd, 1H, Hpyrn-3, J_{H-H} = 4–6 Hz and J_{H-H} = 5–7 Hz); 6.53 (d, 1H, Hpyrn-2, J_{H-H} = 4–6 Hz); 6.38 (d, Hpyrn-6, J_{H-H} = 9–10 Hz); 5.88 (s, 1H, Hpyrz-4); 5.41 (s, 2H, H-CH_2); 2.48 (s, 3H, Hpyrn-CH_3); 2.39 and 2.35 (s, 3H, Hpyrz-5); 2.20 and 2.18 (s, 3H, Hpyrz-3); ^{13}C NMR (CD_2Cl_2, 125 MHz) δ ppm: 156.15 (C-N); 148.33 (Cpyrz-3); 139.56 (Cpyrz-5); 137.56 (Cpyrn-3); 113.25 (Cpyrn-6); 106.96 (Cpyrz-4); 104.69 (1H, Cpyrn-2); 70.67 (2H, CH_2); 23.90 (3H, Cpyrn-CH_3); 13.90 (Cpyrz-3); 10.85 (Cpyrz-5).

N,N-bis((*1H*-pyrazol-1-yl)methyl)thiazol-2-amine (**8**) [80]

2-Aminothiazole (1 g, 9.98 mmol) and (*1H*-pyrazol-1-yl)methanol (1.96 g, 19.97 mmol) were mixed together in acetonitrile (20 mL) under reflux for 4 h, and the solvent was evaporated, then recrystallized in diethyl ether, and then filtrated to obtain the final product: (2.58 g, 99.41%): mp 84–86 °C (diethyl ether); FTIR (KBr, cm^{-1}): 3025 (C-H); 1560 (C=C); 1540 (C-C); 1386 (C-N); 1159 (C=N); 1050 (N-N); 754 (=C-H); 692 (C-S); ^{1}H NMR (CD_2Cl_2, 500 MHz) δ ppm: 7.79 (d, 2H, Hpyrz-5, J_{H-H} = 4–6 Hz); 7.55 (s, 1H, Hthi-2); 7.17 (d, 2H, Hpyrz-3, J_{H-H} = 6–7 Hz); 6.62 (1H, Hthi-5); 6.28 (dd, 2H, Hpyrz-4,); 5.56 (s, 4H, H-CH_2); ^{13}C NMR (CD_2Cl_2, 125 MHz) δ ppm: 167.75 (C-N); 139.80 (2H, Cpyrz-3); 138.79 (1H, Cthi-2); 129.53 (Cpyrz-5); 109.76 (1H, Cthi-5); 105.42 (Cpyrz-4); 59.81 (CH_2).

1-(Bis((*1H*-pyrazol-1-yl)methyl)amino)propan-2-ol (**9**) [81–83]

3-Amino propan-2-ol (1 g, 13.31 mmol) and (3,5-dimethyl-*1H*-pyrazol-1-yl)methanol (3.36 g, 26.62 mmol) were mixed together in acetonitrile (20 mL) under reflux for 4 h, and the solvent was evaporated, then recrystallized in diethyl ether, and then filtrated to obtain the final product: yellow oil; ^{1}H NMR (DMSO-d_6, 400 MHz) δ ppm: 7.58 (d, 3H, Hprop-3 and OH, J_{H-H} = 6–7 Hz); 7.42 (p, 2H, Hpyrz-5, J_{H-H} = 6–8 Hz); 6.24 (d, 2H, Hpyrz-4, J_{H-H} = 5–6 Hz); 4.89 (m, 4H, Hprop-2, J_{H-H} = 5–6 Hz); 4.38 (s, 1H, Hprop-1); 2.46 (d, 2H, CH_2, J_{H-H} = 4–6 Hz); 0.97 (s, 3H, H-CH_3); ^{13}C NMR (DMSO-d_6, 100 MHz) δ ppm: 138.83 (Cpyrz-5); 129.64 (Cpyrz-3); 105.45 (pyrz-4); 66.08 (CH_2); 65.99 (Cprop-2); 54.05 (CH_2); 21.55 (CH_3).

4-(Bis((*1H*-pyrazol-1-yl)methyl)amino)benzonitrile (**10**) [76,84]

4-Aminobenzonitrile (1 g, 8.47 mmol) and (*1H*-pyrazol-1-yl)methanol (1.66 g, 16.94 mmol) were mixed together in acetonitrile (20 mL) under reflux for 4 h, and the solvent was evaporated, then recrystallized in DCM:water (3:1 washed three times in 15:5 mL), and then filtrated to obtain the final product (0.89 g, 96.64%): mp 130–132 °C (diethyl ether); FTIR: 1365.65 cm^{-1} (CN(benzene)); 2218.42 cm^{-1} (C≡N); 2854.74 cm^{-1} (C-H(benzene)); 1455.86 cm^{-1} (C=C(benzene)); 1277.43 cm^{-1} (N-N); 1609.56 cm^{-1} (C=N); 2922.37 cm^{-1}

(C-H (CH2) asym); 2854.03 cm^{-1} (C-H (CH2) sym); 822.486 cm^{-1} (H (benzene)); UV-Visible (λ nm): 201.77 (C=N: Transition n→σ*); 206.78 (C=C: Transition π→π*); 245.24 (C=C: Transition π→π*); 250.74 (C=C: Transition π→π*); 264.74 (C=N: Transition n→π*); ^{1}H NMR (300 MHz, DMSO-d_6) δ ppm: 5.994 (s, 2H, H-CH_2); 6.234 (t, 4H, Hpyrz-4, J_{H-H} = 2–3 Hz); 6.9015 (d, 2H, Hbz-2, J_{H-H} = 6.5–7.5 Hz); 7.36 (d, 2H, Hpyrz-3, J_{H-H} = 9–10 Hz); 7.457 (d, 2H, Hbz-3, J_{H-H} = 9.5–10.5 Hz); 7.8 (d, 2H, Hpyrz-5, J_{H-H} = 8–9 Hz); ^{13}C NMR (75 MHz, DMSO-d_6) δ ppm: 65.58 (C-CH_2); 98.62 (Cbz-1); 105.99 (Cpyrz-4); 113.50 (Cbz-2); 119.90 (Cbz-4); 129.73 (Cpyrz-5); 133.75 (Cbz-3); 139.31 (Cpyrz-3); 150.91 (Cpyrz-5); MS [M^+] (m/z): 278.86 [M^+].

4-(Bis((3,5-dimethyl-*1H*-pyrazol-1-yl)methyl)amino)benzonitrile (**11**) [61,76,84]

4-Aminobenzonitrile (1 g, 8.46 mmol) and 2 equiv. of (3,5-dimethyl-*1H*-pyrazol-1-yl)methanol (2.13 g, 16.92 mmol) were mixed together in acetonitrile (20 mL) under reflux for 4 h, and the solvent was evaporated, then recrystallized in DCM:water (3:1 washed three times in 15:5 mL), and then filtrated to obtain the final product (1.22 g, 86.93%): mp 143–145 °C; FTIR (KBr, ν (cm^{-1})): 1365,65 cm^{-1} (CN (benzene)); 2218.21 cm^{-1} (C≡N); 2854.74 cm^{-1} (C-H(benzene)); 1458.23 cm^{-1} (C=C(benzene)); 1271 cm^{-1} (N-N); 1610.61 cm^{-1} (C=N); 2924.15 cm^{-1} (C-H (CH_2) asym); 2854.74 cm^{-1} (C-H (CH_2) sym); 2934.24 cm^{-1} (C-H (CH_3)); 825.56 cm^{-1} (H (benzene)); UV-Visible (λ nm): 207.77 (C=N: Transition n → σ*); 247.27 (C=C: Transition π →π*); 266.73 (C=N: Transition n →π *); ^{1}H NMR (300 MHz, DMSO-d_6) δ ppm: 6.9425 (d, 2H, Hbz-1, J_{H-H} = 8–9 Hz); 7.485 (d, 2H, Hbz-2, J_{H-H} = 9–10 Hz); 2.26 (s, 2H, Hpyrz-3); 2.477 (s, 2H, Hpyrz-5); 5.779 (s, 2H, Hpyrz-4); 5.33 (d, 4H, H-CH_2, J_{H-H} = 6–7 Hz); ^{13}C NMR (75 MHz, DMSO-d_6) δ ppm: 11.17 (CH_3-5); 13.78 (CH_3-3); 62.87 (C-CH_2); 100.95 (Cbz-1); 106.15 (Cpyrz-4); 113.38 (Cbz-2); 120.02 (Cbz-4); 133.63 (Cbz-3); 139.18 (Cpyrz-5); 146.20 (Cpyrz-3); 151.20 (Cbz-1); MS [M^+] (m/z)**:** 334.8 [M^+].

4-(Bis((3,5-dimethyl-*1H*-pyrazol-1-yl)methyl)amino)benzaldehyde (**12**) [61]

4-Aminobenzaldehyde (1 g, 8.25 mmol) and (3,5-dimethyl-*1H*-pyrazol-1-yl)methanol (2.08 g, 16.5 mmol) were mixed together in acetonitrile (20 mL) under reflux for 4 h, and the solvent was evaporated, then recrystallized in diethyl ether, and then filtrated to obtain the final product (1.8 g, 85%): mp 96–98 °C (diethyl ether); ^{1}H NMR (DMSO-d_6, 500 MHz) δ ppm: 9.69 (s, 1H, OH); 7.71 (d, 2H, Hbz-2, J_{H-H} = 5–6 Hz); 6.81 (d, 2H, Hbz-3, J_{H-H} = 5–6 Hz); 5.83 (s, 2H, Hpyrz-4); 5.24 (s, 4H, H-CH_2); 2.25 (s, 6H, CH_3-5); 2.10 (s, 6H, CH_3-3); ^{13}C NMR (DMSO-d_6, 125 MHz) δ ppm: 189.85 (C=O); 154.21 (Cbz-1); 145.91 (Cbz-3); 138.68 (Cpyrz-3); 131.52 (Cpyrz-5); 124.51 (Cbz-4); 111.05 (Cbz-2); 13.21 (CH_3-3); 10.22 (CH_3-5).

N,*N*-bis((*1H*-pyrazol-1-yl)methyl)-4-nitroaniline (**13**) [61]

4-Nitroaniline (1 g, 7.24mmol) and (*1H*-pyrazol-1-yl)methanol (1.42 g, 14.48 mmol) were mixed together in acetonitrile (20 mL) under reflux for 4 h, and the solvent was evaporated, then recrystallized in diethyl ether, and then filtrated to obtain the final product (0.88 g, 82.05%): mp 86–88 °C (diethyl ether); ^{1}H NMR (DMSO-d_6, 400 MHz) δ ppm: 8.04 (d, 2H, Hbz-2); 7.88 (d, 2H, Hpyrz-5); 7.80 (Hpyrz-3); 6.96 (d, 2H, Hbz-3); 6.28 (t, 2H, Hpyrz-4); 5.61 (s, 4H, H-CH_2); ^{13}C NMR (DMSO-d_6, 100 MHz) δ ppm: 152.82 (Cbz-1); 139.02 (Cpyrz-3); 138.92 (Cbz-4); 129.44 (Cbz-2); 125.85 (Cpyrz-5); 112.13 (Cbz-3); 105.60 (Cpyrz-4); 57.86 (CH_2).

4-(Bis((1*H*-pyrazol-1-yl)methyl)amino)phenol (**14**) [66,69,85–87]

4-Aminophenol (0.9g, 8.24mmol) and (*1H*-pyrazol-1-yl)methanol (1.62 g, 16.49 mmol) were mixed together in acetonitrile (20 mL) under reflux for 4h, and the solvent was evaporated, then recrystallized in diethyl ether, and then filtrated to obtain the final product (1.8 g, 81.1%): mp 102–104 °C (diethyl ether), FTIR (KBr, cm^{-1}): 3113 (O-H); 2300 (C-H); 1659 (C=C); 1509 (C-C); 1393 (C-N); 1183 (C=N); 1039 (N-N); 750 (=C-H), ^{1}H NMR (DMSO, 500 MHz) δ ppm: 8.75 (s, 1H, OH); 7.66 (d, 2H, Hbz-5, J_{H-H} = 4–6 Hz); 7.30 (d, 2H, Hbz-3, J_{H-H} = 5–6 Hz); 7.15 (d, 2H, Hpyrz-5, J_{H-H} = 4–6 Hz); 6.96 (d, 2H, Hpyrz-3, J_{H-H} = 5–7 Hz); 6.31 (dd, 2H, Hpyrz-4, J_{H-H} = 4–6 Hz and J_{H-H} = 6–7 Hz); 5.99 (s, 4H, H-CH_2), ^{13}C NMR

(DMSO, 125 MHz) δ ppm: 167.79 (Cbz-1); 139.68 (Cbz-3); 138.99 (Cbz-1); 130.48 (Cbz-5); 129.32 (Cpyrz-5); 110.42 (Cpyrz-3); 105.91 (Cpyrz-4); 59.09 (CH_2).

4-(Bis((1*H*-pyrazol-1-yl)methyl)amino)benzoic acid (**15**)

4-Aminobenzoic acid (1 g, 7.29 mmol) and (*1H*-pyrazol-1-yl)methanol (1.43 g, 14.58 mmol) were mixed together in acetonitrile (20 mL) under reflux for 4 h, and the solvent was evaporated. then recrystallized in diethyl ether, and then filtrated to obtain the final product (1.24 g, 82.05%): mp 164–166 °C (diethyl ether), FTIR (KBr, cm^{-1}): 3268 (O-H); 1699 (C=O); 1609 (C=C); 1522 (C-C); 1376 (C-N); 1182 (C=N); 951 (N-N); 764 (=C-H), ^{1}H NMR (CD_2Cl_2, 500 MHz) δ ppm: 8.02 (d, 2H, Hbz-3, J_{H-H} = 9–10 Hz); 7.60 (d, 2H, Hpyrz-5, J_{H-H} = 8–10 Hz); 7.55 (d, 2H, Hpyrz-3, J_{H-H} = 5–6 Hz); 7.28 (d, 2H, Hbz-2, J_{H-H} = 5–7 Hz); 6.33 (dd, 2H, Hpyrz-4, J_{H-H} = 6–8 Hz and J_{H-H} = 14–15 Hz); 5.88 (s, 4H, H-CH_2), ^{13}C NMR (CD_2Cl_2, 125 MHz) δ ppm: 140.03 (Cbz-1); 139.96 (Cpyrz-3); 132 (Cbz-2); 128.88 (Cpyrz-5); 113,74 (Cbz-4); 112.62 (Cbz-3); 106.36 (Cpyrz-4); 66.69 (C-CH_2). The elemental Analysis was calculated for $C_{15}H_{15}N_5O_2$ (M.wt 297.12); C-60.60, H-5.09, and N-23.56 were the % calculated. C-60.58; H-5.12; and N-23.45 were the % found.

3.3. Biological Evaluation

3.3.1. Antibacterial Assay

The microdilution method with phenol red [88] evaluated the antibacterial effect against four bacterial strains: *Listeria monocytogenes*, *Escherichia coli*, *Staphylococcus aureus, and Citrobacter freundii*. First, the bacterial isolate was cultivated in liquid Luria–Bertani medium (LB) overnight at 37 °C under aeration. Then, a suspension containing 10^6 CFU/mL of bacteria cells was prepared. Next, an aliquot from this bacterial suspension was added to test tubes containing phenol red medium and the compound to be tested. After an incubation of 24 h at 37 °C, the color of the culture remains red in the absence of growth, indicating that the tested compound has antibacterial activity against the tested strain. However, if there is bacterial growth, the culture becomes yellow due to the acidification of the medium and indicating that the tested compound lacks antibacterial activity against the tested strain. All the experiments were repeated twice for each drug, including the antibiotic streptomycin as a positive control, and means were calculated.

3.3.2. Determination of the Minimum Inhibitory Concentration (MIC) and the Minimum Bactericidal Concentration (MBC)

The MIC (the lowest drug concentration that inhibits bacterial growth after incubation at 37 °C for 24 h) and the MBC (the lowest drug concentration that kills 99% of bacteria after 24 h of incubation) were obtained as described in the literature [89,90].

3.3.3. Antifungal Assay

The prepared ligands were evaluated for their antifungal activity using liquid cell culture against *Saccharomyces cerevisiae* and Candida species: *Candida glabrata* and *Candida albicans*. The growth rate of fungal cells in liquid culture was monitored by absorbance measurements at 600 nm (OD_{600}) using a V-1200 spectrophotometer (Shanghai Mapada Instruments Co., Ltd., Shanghai, China). The antifungal activity was described (Bouchal et al., 2019 [88]). Briefly, cells were cultured in the presence and absence of 500 µM of each compound for 24 h, and OD600 measurements were then used to monitor the growth rate. Growth in the presence of a compound was expressed as a percentage relative to the untreated control. All experiments were repeated at least twice, and means were calculated.

3.4. Computational Studies

3.4.1. In Silico ADME-Tox Predictions

In silico screening was performed to predict the studied compounds' properties (absorption, distribution, metabolism, excretion) of the ADME [9,88,91–104]

Additionally, using the SwissADME web tool (www.swissadme.ch/, accessed on 20 April 2022) [105–107], lipophilicity (*logP*) was calculated using the Marvin sketch

program, while the toxicity predictions were made using the PROTOX online tool (http://tox.charite.de/protox_II/, accessed on 20 April 2022) [108–113] based on the functional group similarity of the existing molecules tested in vitro and in vivo in the database. The three most similar compounds were taken for toxicity prediction.

3.4.2. DFT, Molecular Ligand–Protein Docking, and Virtual Screening Studies

The chemical structures of the studied molecules were sketched using Gaussview 6.0, then optimized using the DFT/B3LYP method with 6-31G(d,p) basis sets in the Gaussian 09W software [114]. The docking study performed with New Delhi metallo-β-lactamase was conducted in two different active sites of the crystal structure of NDM-1 at pH 5.5 (Bis-Tris) in a complex with hydrolyzed Ampicillin (**PDB: 5ZGE**) with a resolution of 1.00 Å.

Blind docking/virtual screening was considered to target the previous protein (5ZGE), which was prepared in Autodock 4 [115] default parameters, and the whole protein was used for the grid box (Table S1), with Perl as a launcher for all the ligands in Autodock Vina [116–120].

4. Conclusions

Fifteen compounds based on pyrazole derivatives were prepared with good yield and characterized using different physicochemical analyses, such as FTIR, UV-Visible, ^{1}H and ^{13}C NMR, and MS. These compounds were evaluated for their antifungal and antibacterial activities against several fungal and bacterial strains. None of the compounds had antifungal activity. Interestingly, compounds **12** and **14** displayed intense antibacterial activity. In addition, compound **12** presented excellent antibacterial activity against *E. coli*, *S. aureus*, and *C. freundii*, with inactivity against *L. monocytogenes* and cephalosporins antibiotics. In contrast, compound **14** showed tremendous antibacterial potential against *L. monocytogenes*, with no effect against the other bacterial strains.

Compound **14**'s listericidal activity could be due to the presence of the hydroxyl as a substituent on the phenyl ring, an electron donor group (+M) that causes oxidative stress to the bacterial strain the production of hydroxyl radicals. In contrast, compound **12** has carbonyl as an electron-withdrawing group (-M), methyl as an electron donor group (+I), and a bulky substituent. Furthermore, from the MEP surface analysis, compound **12** only has a higher negative charge value over the carbonyl. In contrast, compound **14,** similar to the antibiotics cefotaxime and Ampicillin, has a close negative-positive (δ^{+}-δ^{-}) higher charge value over the hydroxyl and the acidic function.

From ADME and toxicity predictions, compounds **12** and **14** have no violations of Lipinski's rule of five, better than streptomycin, with three violations, and cefotaxime, with one offense. In contrast, compounds **12** and **14** have lower predicted LD_{50} than Ampicillin and cefotaxime, with less toxicity (class 4) than streptomycin (class 3), even though they are both active as carcinogens with mutagenic activity for compound **14** and have no binding probability with all the toxicity targets better than Ampicillin and cefotaxime, which have probable binding with toxicity targets.

From the docking results, compound **12** has a better affinity with both active protein sites, which have an H-acceptor bond, than compound **14**, with ligand exposure. However, Ampicillin and cefotaxime still have the best values, with more H-donors and H-acceptors; otherwise, compound **12** is hydrolyzed by NDM1 hydrolysis and inactivates its antibacterial activity against *Listeria monocytogenes* due to the presence of the carbonyl function, which is common in all β-lactam antibiotics. On the other hand, compound **14** has listericidal activity with a specific mechanism that needs more computational studies and biological assays for prediction; from blind docking/virtual screening studies, the mode of binding interaction is the same as that of LYS216, which is bound with the nitrogen of pyrazole for the ligand **12** and the oxygen for Ampicillin with the same binding affinity of −7.1 Kcal/mol. On the other hand, ligand **14** has a lower −7.0 Kcal/mol value with amino acids such as ILE203 and LYS242.

Supplementary Materials: The following are available online at https://www.mdpi.com/article/10.3390/ph15070803/s1, Table S1: Blind docking/virtual screening as Perl configuration and GRID box parameters; File S1: ^{1}HNMR and ^{13}CNMR spectra of compounds.

Author Contributions: Y.K. methodology, formal analysis, software, resources, original draft preparation, writing—review and editing. M.B. validation, investigation, and visualization. F.A. software, data curation, and resources. M.E.K. software, data curation, supervision, A.E., validation, formal analysis, and funding acquisition, and R.T. supervision, validation, and conceptualization. M.H.A. visualization, writing—review and editing, and funding acquisition. All authors have read and agreed to the published version of the manuscript.

Funding: This research was funded by MESRSFC (Ministère de l'Enseignement Supérieur, de la Recherche Scientifique et de la Formation des Cadres), the CNRST (Center National pour la Recherche Scientifique et Technique) and Taif University, Taif, Saudi Arabia (grant number TURSP2020/91).

Institutional Review Board Statement: Not applicable.

Informed Consent Statement: Not applicable.

Data Availability Statement: Data are contained within the article and supplementary material.

Conflicts of Interest: The authors declare no conflict of interest.

References

1. Lu, Z.; Wanang, H.; Zhang, A.; Liu, X.; Zhou, W.; Yang, C.; Guddat, L.; Yang, H.; Schofield, C.J.; Rao, Z. Structures of Mycobacterium tuberculosis Penicillin-Binding Protein 3 in Complex with Five beta-Lactam Antibiotics Reveal Mechanism of Inactivation. *Mol. Pharmacol.* **2020**, *97*, 287–294. [CrossRef]
2. Antipin, R.L.; Beshnova, D.A.; Petrov, R.A.; Shiryaeva, A.S.; Andreeva, I.P.; Grigorenko, V.G.; Rubtsova, M.Y.; Majouga, A.G.; Lamzin, V.S.; Egorov, A.M. Synthesis, SAR and molecular docking study of novel non-beta-lactam inhibitors of TEM type beta-lactamase. *Bioorganic Med. Chem. Lett.* **2017**, *27*, 1588–1592. [CrossRef]
3. Kogut, M.; Harris, M. Effects of Streptomycin in Bacterial Cultures Growing at Different Rates; Interaction with Bacterial Ribosomes in vivo. *Eur. J. Biochem.* **1969**, *9*, 42–49. [CrossRef]
4. Mazumdar, K.; Dastidar, S.G.; Park, J.H.; Dutta, N.K. The anti-inflammatory non-antibiotic helper compound diclofenac: An antibacterial drug target. *Eur. J. Clin. Microbiol. Infect. Dis.* **2009**, *28*, 881–891. [CrossRef]
5. Chudobova, D.; Dastidar, S.G.; Park, J.H.; Dutta, N.K. Effect of Ampicillin, streptomycin, penicillin and tetracycline on metal resistant and non-resistant Staphylococcus aureus. *Int. J. Environ. Res. Public Health* **2014**, *11*, 3233–3255. [CrossRef]
6. Hoerr, V.; Duggan, G.E.; Zbytnuik, L.; Poon, K.K.H.; Grobe, C.; Neugebauer, U.; Methling, K.; Loffler, B.; Vogel, H.J. Characterization and prediction of the mechanism of action of antibiotics through NMR metabolomics. *BMC Microbiol.* **2016**, *16*, 82. [CrossRef]
7. Stern, A.L.; Van der Verren, S.E.; Näsvall, J.; Gutiérrez-de-Terán, H.; Selmer, M. Structural mechanism of AadA, a dual-specificity aminoglycoside adenylyltransferase from Salmonella enterica. *J. Biol. Chem.* **2018**, *293*, 11481–11490. [CrossRef]
8. Cho, S.; Hiott, L.M.; Barrett, J.B.; McMillan, E.A.; House, S.L.; Humayoun, S.B.; Adams, E.S.; Jackson, C.R.; Frye, J.G. Prevalence and characterization of Escherichia coli isolated from the Upper Oconee Watershed in Northeast Georgia. *PLoS ONE* **2018**, *13*, e0197005. [CrossRef]
9. Bendaif, H.; Melhaoui, A.; Ramdani, M.; Elmsellem, H.; Douez, C.; El Ouadi, Y. Antibacterial activity and virtual screening by molecular docking of lycorine from Pancratium foetidum Pom (Moroccan endemic Amaryllidaceae). *Microb. Pathog.* **2018**, *115*, 138–145. [CrossRef]
10. Alexandre, H.L.; Kuzin, P.; Kelly, J.A.; Knox, J.R. Binding of Cephalothin and Cefotaxime to D-Ala-D-Ala-Peptidase Reveals a Functional Basis of a Natural Mutation in a Low-Affinity Penicillin-Binding Protein and in Extended-Spectrum P-Lactamases. *Biochemistry* **1995**, *34*, 9532–9540.
11. Pacifici, G.M.; Marchini, G. Clinical Pharmacology of Cefotaxime in Neonates and Infants: Effects and Pharmacokinetics. *Int. J. Pediatr.* **2017**, *5*, 6111–6138.
12. Wangoye, K.; Mwesigye, J.; Tungotyo, M.; Twinomujuni Samba, S. Chronic wound isolates and their minimum inhibitory concentrations againgst third generation cephalosporins at a tertiary hospital in Uganda. *Sci. Rep.* **2022**, *12*, 1195. [CrossRef]
13. Shahbaz, K. Cephalosporins: Pharmacology and chemistry. *Pharm. Biol. Eval.* **2017**, *4*, 234–238. [CrossRef]
14. Mohamed, S.B.; Adlan, T.A.; Khalafalla, N.A.; Abdall, N.I.; Ali, Z.S.A.; Ka, A.M.; Hassan, M.M.; Elnour, M.A.B. Proteomics and Docking Study Targeting Penicillin-Binding Protein and Penicillin-Binding Protein2a of Methicillin-Resistant *Staphylococcus aureus* Strain SO-1977 Isolated from Sudan. *Evol. Bioinform.* **2019**, *15*, 1–13. [CrossRef]
15. Dhara, L.; Tripathi, A.; Pal, A. Molecular characterization and in silico analysis of naturally occurring TEM beta-lactamase variants among pathogenic Enterobacteriaceae infecting Indian patients. *BioMed Res. Int.* **2013**, *2013*, 783540. [CrossRef]

16. Danishuddin, M.; Khan, A.U. Molecular modeling and docking analysis of beta-lactamases with inhibitors: A comparative study. *Silico Biol.* **2011**, *11*, 273–280.
17. Thakur, P.K.; Kumar, J.; Ray, D.; Anjum, F.; Hassan, M.I. Search of potential inhibitor against New Delhi metallo-beta-lactamase 1 from a series of antibacterial natural compounds. *J. Nat. Sci. Biol. Med.* **2013**, *4*, 51–56.
18. Temple, M.E.; Nahata, M.C. Treatment of listeriosis. *Ann. Pharmacother.* **2000**, *34*, 656–661. [CrossRef]
19. Ahrén, I.L.; Karlsson, E.; Forsgren, A.; Riesbeck, K. Comparison of the antibacterial activities of Ampicillin, ciprofloxacin, clarithromycin, telithromycin and quinupristin/dalfopristin against intracellular non-typeable Haemophilus influenzae. *J. Antimicrob. Chemother.* **2002**, *50*, 903–906. [CrossRef]
20. Sutherland, R.; Rolinson, G.N. Activity of Ampicillin in vitro compared with other antibiotics. *J. Clin. Pathol.* **1964**, *17*, 461–465. [CrossRef]
21. Rao, L.; Tian, R.; Chen, X. Cell-Membrane-Mimicking Nanodecoys against Infectious Diseases. *ACS Nano* **2020**, *14*, 2569–2574. [CrossRef] [PubMed]
22. Lungu, B.; O'Bryan, C.A.; Muthaiyan, A.; Milillo, S.R.; Johnson, M.G.; Crandall, P.G.; Ricke, S.C. Listeria monocytogenes: Antibiotic resistance in food production. *Foodborne Pathog. Dis.* **2011**, *8*, 569–578. [CrossRef] [PubMed]
23. Koster, S.; van Pee, K.; Hudel, M.; Leustik, M.; Rhinow, D.; Kuhlbrandt, W.; Chakraborty, T.; Yildiz, O. Crystal structure of listeriolysin O reveals molecular details of oligomerization and pore formation. *Nat. Commun.* **2014**, *5*, 3690. [CrossRef]
24. Radoshevich, L.; Cossart, P. Listeria monocytogenes: Towards a complete picture of its physiology and pathogenesis. *Nat. Rev. Microbiol.* **2018**, *16*, 32–46. [CrossRef]
25. Lv, H.; Ning, B. Pathogenesis of bloodstream infection in children with blood cancer. *Exp. Ther. Med.* **2013**, *5*, 201–204. [CrossRef]
26. Anufrieva, N.V.; Faleev, N.G.; Morozova, E.A.; Bazhulina, N.P.; Revtovich, S.V.; Timofeev, V.P.; Tkachev, Y.V.; Nikulin, A.D.; Demidkina, T.V. The role of active site tyrosine 58 in Citrobacter freundii methionine γ-lyase. *Biochim. Biophys. Acta* **2015**, *1854*, 1220–1228. [CrossRef] [PubMed]
27. Morozova, E.A.; Bazhulina, N.P.; Anufrieva, N.V.; Mamaeva, D.V.; Tkachev, Y.V.; Streltsov, S.A.; Timofeev, V.P.; Faleev, N.G.; Demidkina, T.V. Kinetic and spectral parameters of interaction of Citrobacter freundii methionine γ-lyase with amino acids. *Biochemistry* **2010**, *75*, 1272–1280. [CrossRef]
28. Revtovich, S.V.; Morozova, E.A.; Kulikova, V.V.; Anufrieva, N.V.; Osipova, T.I.; Koval, V.S.; Nikylin, A.D.; Demidkima, T.V. Crystal structure of mutant form Cys115His of Citrobacter freundii methionine γ-lyase complexed with L-norleucine. *Biochim. Biophys. Acta Proteins Proteom.* **2017**, *1865*, 1123–1128. [CrossRef]
29. Liu, L.H.; Wang, N.Y.; Wu, A.Y.; Lin, C.C.; Lee, C.M.; Liu, C.P. Citrobacter freundii bacteremia: Risk factors of mortality and prevalence of resistance genes. *J. Microbiol. Immunol. Infect.* **2018**, *51*, 565–572. [CrossRef]
30. Munoz, P.; Bouza, E.; Cuenca-Estrella, M.; Eiros, J.M.; Perez, M.J.; Sanchez-Somolinos, M.; Rincon, C.; Hortal, J.; Pelaez, T. Saccharomyces cerevisiae fungemia: An emerging infectious disease. *Clin. Infect. Dis.* **2005**, *40*, 1625–1634. [CrossRef]
31. Fidel, P.L.; Vazquez, J.A.; Sobel, J.D. Candida glabrata: Review of Epidemiology, Pathogenesis, and Clinical Disease with Comparison toC. Albicans. *Clin. Microbiol. Rev.* **1999**, *12*, 80–96. [CrossRef]
32. Wu, D.; Jin, F.; Lu, W.; Zhu, J.; Li, C.; Wang, W.; Tang, Y.; Jiang, H.; Huang, J.; Liu, G.; et al. Synthesis, structure-activity relationship, and pharmacophore modeling studies of pyrazole-3-carbohydrazone derivatives as dipeptidyl peptidase IV inhibitors. *Chem. Biol. Drug Des.* **2012**, *79*, 897–906. [CrossRef] [PubMed]
33. Tighadouini, S.; Benabbes, R.; Tillard, M.; Eddike, D.; Haboubi, K.; Karrouchi, K.; Radi, S. Synthesis, crystal structure, DFT studies and biological activity of (Z)-3-(3-bromophenyl)-1-(1,5-dimethyl-1H-pyrazol-3-yl)-3-hydroxyprop-2-en-1-one. *Chem. Cent. J.* **2018**, *12*, 122. [CrossRef] [PubMed]
34. Barakat, A.; Al-Majid, A.M.; Al-Qahtany, B.M.; Ali, M.; Teleb, M.; Al-agamy, M.H.; Naz, S.; Ul-Haq, Z. Synthesis, antimicrobial activity, pharmacophore modeling and molecular docking studies of new pyrazole-dimedone hybrid architectures. *Chem. Cent. J.* **2018**, *12*, 29. [CrossRef] [PubMed]
35. Karrouchi, K.; Radi, S.; Ramli, Y.; Taoufik, J.; Mabkhot, Y.N.; Al-Aizari, F.A.; Ansar, M. Synthesis and Pharmacological Activities of Pyrazole Derivatives: A Review. *Molecules* **2018**, *23*, 134. [CrossRef] [PubMed]
36. Rao, A.B.P.; Gulati, K.; Joshi, N.; Deb, D.K.; Rambabu, D.; Kaminsky, W.; Poluri, K.M.; Kollipara, M.R. Synthesis and biological studies of ruthenium, rhodium and iridium metal complexes with pyrazole-based ligands displaying unpredicted bonding modes. *Inorg. Chim. Acta* **2017**, *462*, 223–235.
37. Bekhit, A.A.; Hymete, A.; Asfaw, H.; Ael, D.B. Synthesis and biological evaluation of some pyrazole derivatives as anti-malarial agents. *Arch. Pharm.* **2012**, *345*, 147–154. [CrossRef]
38. El Shehry, M.F.; Ghorab, M.M.; Abbas, S.Y.; Fayed, E.A.; Shedid, S.A.; Ammar, Y.A. Quinoline derivatives bearing pyrazole moiety: Synthesis and biological evaluation as possible antibacterial and antifungal agents. *Eur. J. Med. Chem.* **2018**, *143*, 1463–1473. [CrossRef]
39. Brahmbhatt, G.C.; Sutariya, T.R.; Atara, H.D.; Parmar, N.J.; Gupta, V.K.; Lagunes, I.; Padrón, J.M.; Murumkar, P.R.; Yadav, M.R. New pyrazolyl-dibenzo[b,e][1,4]diazepinones: Room temperature one-pot Synthesis and biological evaluation. *Mol. Divers.* **2020**, *24*, 355–377. [CrossRef]
40. Dai, H.; Chen, J.; Li, G.; Ge, S.; Shi, Y.; Fang, Y.; Ling, Y. Design, Synthesis, and bioactivities of novel oxadiazole-substituted pyrazole oximes. *Bioorganic Med. Chem. Lett.* **2017**, *27*, 950–953. [CrossRef]

41. Aggarwal, R.; Kumar, V.; Kumar, R.; Singh, S.P. Approaches towards the Synthesis of 5-aminopyrazoles. *Beilstein J. Org. Chem.* **2011**, *7*, 179–197. [CrossRef] [PubMed]
42. Aggarwal, R.; Kumar, S. 5-Aminopyrazole as precursor in design and Synthesis of fused pyrazoloazines. *Beilstein J. Org. Chem.* **2018**, *14*, 203–242. [CrossRef]
43. Kaddouri, Y.; Abrigach, F.; Yousfi, E.B.; El Kodadi, M.; Touzani, R. New thiazole, pyridine and pyrazole derivatives as antioxidant candidates: Synthesis, DFT calculations and molecular docking study. *Heliyon* **2020**, *6*, e03185. [CrossRef] [PubMed]
44. Elshaier, Y.A.; Barakat, A.; Al-Qahtany, B.M.; Al-Majid, A.M.; Al-Agamy, M.H. Synthesis of Pyrazole-Thiobarbituric Acid Derivatives: Antimicrobial Activity and Docking Studies. *Molecules* **2016**, *21*, 1337. [CrossRef] [PubMed]
45. Brahmbhatt, H.; Molnar, M.; Pavić, V. Pyrazole nucleus fused tri-substituted imidazole derivatives as antioxidant and antibacterial agents. *Karbala Inter. J. Moder. Sci.* **2018**, *4*, 200–206. [CrossRef]
46. Abrigach, F.; Rokni, Y.; Takfaoui, A.; Khoutoul, M.; Doucet, H.; Asehraou, A.; Touzani, R. In vitro screening, homology modeling and molecular docking studies of some pyrazole and imidazole derivatives. *Biomed. Pharmacother.* **2018**, *103*, 653–661. [CrossRef]
47. Govender, H.; Mocktar, C.; Kumalo, H.M.; Koorbanally, N.A. Synthesis, antibacterial activity and docking studies of substituted quinolone thiosemicarbazones. *Phosphorus Sulfur Silicon Relat. Elem.* **2019**, *194*, 1074–1081. [CrossRef]
48. Chandrasekar, K.; Kumar, B.; Saravanan, A.; Victor, A.; Sivaraj, S.; Haridoss, M.; Priyadurairaj, P.; Hemalatha, C.N.; Muthukumar, V.A. Evalution and Molecular Docking of Benzimidazole and its Derivatives as a Potent Antibacterial Agent. *Biomed. Pharmacol. J.* **2019**, *12*, 1835–1847. [CrossRef]
49. Grein, F.; Schneider, T.; Sahl, H.G. Docking on Lipid II—A Widespread Mechanism for Potent Bactericidal Activities of Antibiotic Peptides. *J. Mol. Biol.* **2019**, *431*, 3520–3530. [CrossRef]
50. Hassan, A.S.; Askar, A.A.; Nossier, E.S.; Naglah, A.M.; Moustafa, G.O.; Al-Omar, M.A. Antibacterial Evaluation, In Silico Characters and Molecular Docking of Schiff Bases Derived from 5-aminopyrazoles. *Molecules* **2019**, *24*, 3130. [CrossRef]
51. Al-Khafaji, K.; Taskin Tok, T. Understanding the mechanism of amygdalin's multifunctional anti-cancer action using computational approach. *J. Biomol. Struct. Dyn.* **2021**, *39*, 1600–1610. [CrossRef] [PubMed]
52. Ghorab, M.M.; Soliman, A.M.; Alsaid, M.S.; Askar, A.A. Synthesis, antimicrobial activity and docking study of some novel 4-(4,4-dimethyl-2,6-dioxocyclohexylidene)methylamino derivatives carrying biologically active sulfonamide moiety. *Arab. J. Chem.* **2020**, *13*, 545–556. [CrossRef]
53. Rezki, N.; Al-blewi, F.F.; Al-Sodies, S.A.; Alnuzha, A.K.; Messali, M.; Ali, I.; Aouad, M.R. Synthesis, Characterization, DNA Binding, Anticancer, and Molecular Docking Studies of Novel Imidazolium-Based Ionic Liquids with Fluorinated Phenylacetamide Tethers. *ACS Omega* **2020**, *5*, 4807–4815. [CrossRef]
54. Zhang, F.; Zhai, T.; Haider, S.; Liu, Y.; Huang, Z.J. Synergistic Effect of Chlorogenic Acid and Caffeic Acid with Fosfomycin on Growth Inhibition of a Resistant Listeria monocytogenes Strain. *ACS Omega* **2020**, *5*, 7537–7544. [CrossRef] [PubMed]
55. Gurung, A.B.; Ali, M.A.; Lee, J.; Al-Hemaid, F.; Abul Farah, M.; Al-Anazi, K.M. Molecular docking elucidates the plausible mechanisms underlying the anticancer properties of acetyldigitoxigenin from Adenium obesum. *Saudi J. Biol. Sci.* **2020**, *27*, 1907–1911. [CrossRef] [PubMed]
56. Gowda, K.; Swarup, H.A.; Nagarakere, S.C.; Rangappa, S.; Kanchugarkoppal, R.S.; Kempegowda, M. Structural studies of 2,5-disubstituted 1,3,4-thiadiazole derivatives from dithioesters under the mild condition: Studies on antioxidant, antimicrobial activities, and molecular docking. *Synth. Commun.* **2020**, *50*, 1528–1544. [CrossRef]
57. Abusetta, A.; Alumairi, J.; Alkaabi, M.Y.; Al Ajeil, R.; Abu Shkaidim, A.; Akram, D.; Pajak, J.; Ghattas, M.A.; Atatreh, N.; AlNeyadi, S.S. Design, Synthesis, in Vitro Antibacterial Activity, and Docking Studies of New Rhodanine Derivatives. *Open J. Med. Chem.* **2020**, *10*, 15–34.
58. Zhang, H.; Ma, G.; Zhu, Y.; Zeng, L.; Ahmad, A.; Wang, C.; Pang, B.; Fang, H.; Zhao, L.; Hao, Q. Active-Site Conformational Fluctuations Promote the Enzymatic Activity of NDM-1. *Antimicrob. Agents Chemother.* **2018**, *62*, e01579-18. [CrossRef]
59. Sun, Z.; Hu, L.; Sankaran, B.; Prasad, B.V.V.; Palzkill, T. Differential active site requirements for NDM-1 beta-lactamase hydrolysis of carbapenem versus penicillin and cephalosporin antibiotics. *Nat. Commun.* **2018**, *9*, 4524. [CrossRef]
60. El Kodadi, M.; Malek, F.; Touzani, R.; Ramdani, A. Synthesis of new tripodal ligand 5-(bis(3,5-dimethyl-1H-pyrazol-1-ylmethyl)amino)pentan-1-ol, catecholase activities studies of three functional tripodal pyrazolyl N-donor ligands, with different copper (II) salts. *Catal. Commun.* **2008**, *9*, 966–969. [CrossRef]
61. Kaddouri, Y.; Abrigach, F.; Ouahhoud, S.; Benabbes, R.; El Kodadi, M.; Alsalme, A.; Al-Zaqri, N.; Warad, I.; Touzani, R. Synthesis, characterization, reaction mechanism prediction and biological study of mono, bis and tetrakis pyrazole derivatives against Fusarium oxysporum f. sp. Albedinis with conceptual DFT and ligand-protein docking studies. *Bioorganic Chem.* **2021**, *110*, 104696. [CrossRef] [PubMed]
62. Touzani, R.; Ramdani, A.; Ben-Hadda, T.; El Kadiri, S.; Maury, O.; Le Bozec, H.; Dixneuf, P.H. Efficient synthesis of new nitrogen donor containing tripods under microwave irradiation and without solvent. *Synth. Commun.* **2001**, *31*, 1315–1321. [CrossRef]
63. Lamsayah, M.; Khoutoul, M.; Abrigach, F.; Oussaid, A.; Touzani, R. Selective liquid-liquid extraction of Fe(II) and Cd(II) using N,N'-Pyrazole bidentate ligands with theoretical study investigations. *Separ. Sci. Technol.* **2015**, *50*, 2170–2176.
64. Khoutoul, M.; Abrigach, F.; Zarrouk, A.; Benchat, N.-E.; Lamsayah, M.; Touzani, R. New nitrogen-donnor pyrazole ligands for excellent liquid-liquid extraction of Fe^{2+} ions from aqueous solution, with theoretical study. *Res. Chem. Interm.* **2015**, *41*, 3319–3334. [CrossRef]

65. Garbacia, S.; Hillairet, C.; Touzani, R.; Lavastre, O. New nitrogen-rich tripodal molecules based on bis(pyrazol-1-ylmethyl)amines with substituents modulating steric hindrances and electron density of donor sites. *Collect. Czechoslov. Chem. Commun.* **2005**, *70*, 34–40. [CrossRef]
66. Bouabdallah, I.; Touzani, R.; Zidane, I.; Ramdani, A. Synthesis of new tripodal ligand: N,N-bis[(1,5-dimethylpyrazol-3-yl)methyl]benzylamine. Catecholase activity of two series of tripodal ligands with some copper (II) salts. *Catal. Commun.* **2007**, *8*, 707–712. [CrossRef]
67. El Kodadi, M.; Benamar, M.; Ibrahim, B.; Zyad, A.; Malek, F.; Touzani, R.; Ramdani, A.; Melhaoui, A. New Synthesis of two tridentate bipyrazolic compounds and their cytotoxic activity tumor cell lines. *Nat. Prod. Res.* **2007**, *21*, 947–952. [CrossRef]
68. Touzani, R.; Garbacia, S.; Lavastre, O.; Yadav, V.K.; Carboni, B. Efficient solution phase combinatorial access to a library of pyrazole- and triazole-containing compounds. *J. Comb. Chem.* **2003**, *5*, 375–378. [CrossRef]
69. Touzani, R.; Vasapollo, G.; Scorrano, S.; Del Sole, R.; Manera, M.G.; Rella, R.; El Kadiri, S. New complexes based on tridentate bispyrazole ligand for optical gas sensing. *Mater. Chem. Phys.* **2011**, *126*, 375–380. [CrossRef]
70. Boussalah, N.; Touzani, R.; Bouabdallah, I.; El Kadiri, S.; Ghalem, S. Oxidation catalytic properties of new amino acid based on pyrazole tripodal ligands. *Inter. J. Acad. Res.* **2009**, *1*, 137–143.
71. Boussalah, N.; Touzani, R.; Bouabdallah, I.; El Kadiri, S.; Ghalem, S. Synthesis, structure and catalytic properties of tripodal amino-acid derivatized pyrazole-based ligands. *J. Mol. Catal. A Chem.* **2009**, *306*, 113–117. [CrossRef]
72. Hammouti, B.; Dafali, A.; Touzani, R.; Bouachrine, M. Inhibition of copper corrosion by bipyrazole compound in aerated 3% NaCl. *J. Saudi Chem. Soc.* **2012**, *16*, 413–418. [CrossRef]
73. Boussalah, N.; Touzani, R.; Souna, F.; Himri, I.; Bouakka, M.; Hakkou, A.; Ghalem, S.; El Kadiri, S. Antifungal activities of amino acid ester functional pyrazolyl compounds against Fusarium oxysporum f.sp. albedinis and Saccharomyces cerevisiae yeast. *J. Saudi Chem. Soc.* **2013**, *17*, 17–21. [CrossRef]
74. Abrigach, F.; Bouchal, B.; Riant, O.; Mace, Y.; Takfaoui, A.; Radi, S.; Oussaid, A.; Bellaoui, M.; Touzani, R. New N,N,N′,N′-tetradentate Pyrazoly Agents: Synthesis and Evaluation of their Antifungal and Antibacterial Activities. *Med. Chem.* **2016**, *12*, 83–89. [CrossRef]
75. Abrigach, F.; Karzazi, Y.; Benabbes, R.; El Youbi, M.; Khoutoul, M.; Taibi, N.; Karzazi, N.; Benchat, N.; Bouakka, M.; Saalaoui, E.; et al. Synthesis, biological screening, POM, and 3D-QSAR analyses of some novel pyrazolic compounds. *Med. Chem. Res.* **2017**, *26*, 1784–1795. [CrossRef]
76. Kaddouri, Y.; Abrigach, F.; Mechbal, N.; Karzazi, Y.; El Kodadi, M.; Aouniti, A.; Touzani, R. Pyrazole Compounds: Synthesis, molecular structure, chemical reactivity, experimental and theoretical DFT FTIR spectra. *Mater. Today Proc.* **2019**, *13*, 956–963. [CrossRef]
77. El Ati, R.; Takfaoui, A.; El Kodadi, M.; Touzani, R.; Yousfi, E.B.; Almalki, A.A.; Ben Hadda, T. Catechol oxidase and Copper(I/II) Complexes Derived from Bipyrazol Ligand: Synthesis, Molecular Structure Investigation of New Biomimetic Functional Model and Mechanistic Study. *Mater. Today Proc.* **2019**, *13*, 129–1237. [CrossRef]
78. Toubi, Y.; Touzani, R.; Radi, S.; El Kadiri, S. Synthesis, characterization and catecholase activity of copper (II) complexes with bispyrazole tri-podal ligands. *J. Mater. Environ. Sci.* **2012**, *3*, 328–341.
79. Radi, S.; Toubi, Y.; Draoui, N.; Feron, O.; Riant, O. One-pot synthesis and in vitro antitumor activity of some bipyrazolic tripodal derivatives. *Lett. Drug Des. Disc.* **2012**, *9*, 305–309.
80. Kalanithi, M.; Rajarajan, M.; Tharmaraj, P.; Johnson Raja, S. Synthesis, spectroscopic characterization, analgesic, and antimicrobial activities of Co(II), Ni(II), and Cu(II) complexes of 2-[N,N-bis-(3,5-dimethyl-pyrazolyl-1- methyl)]aminothiazole. *Med. Chem. Res.* **2015**, *24*, 1578–1585. [CrossRef]
81. Ghosh, D.; Kundu, N.; Maity, G.; Choi, K.-Y.; Caneschi, A.; Endo, A.; Chaudhury, M. Synthesis, Structure, Magnetism, and Spectroscopic Properties of Heterobinuclear Copper(II)-Zinc(II) Complexes and Their Copper(II)-Copper(II) Analogues in Asymmetric Ligand Environments. *Inorg. Chem.* **2004**, *43*, 6015–6023. [CrossRef] [PubMed]
82. Malek, F.; Draoui, N.; Feron, O.; Radi, S. Tridentate bipyrazole compounds with a side-arm as a new class of antitumor agents. *Res. Chem. Intermed.* **2014**, *40*, 681–687. [CrossRef]
83. Harit, T.; Cherfi, M.; Isaad, J.; Riahi, A.; Malek, F. New generation of functionalized bipyrazolic tripods: Synthesis and study of their coordination properties towards metal cations. *Tetrahedron* **2012**, *68*, 4037–4041. [CrossRef]
84. Kaddouri, Y.; Takfaoui, A.; El Ati, R.; Abrigach, F.; Lamsayah, M.; Touzani, R. Synthesis of four new tridentate pyrazolic ligands. *J. Mar. Chim. Heter.* **2017**, *16*, 100–104.
85. Bouabdallah, I.; Touzani, R.; Zidane, I.; Ramdani, A.; Jalbout, A.F.; Trzaskowski, B. New comparative theoretical calculations of some N,N-bis[(3,5-dimethylpyrazol-1-yl)methyl]phenylamines tripodal ligands. *J. Mater. Environ. Sci.* **2013**, *4*, 671–674.
86. Touzani, R.; El Kadiri, S.; Zerrouki, A.; Scorrano, S.; Vasapollo, G.; Manera, M.G.; Casino, F.; Rella, R. Optical and morphological characterization of bispyrazole thin films for gas sensing applications. *Arab. J. Chem.* **2014**, *7*, 695–700. [CrossRef]
87. Mouadili, A.; Attayibat, A.; El Kadiri, S.; Radi, S.; Touzani, R. Catecholase activity investigations using in situ copper complexes with pyrazole and pyridine based ligands. *Appl. Catal. A* **2013**, *454*, 93–99. [CrossRef]
88. Bouchal, B.; Abrigach, F.; Takfaoui, A.; Errahhali, M.E.; Errahhali, M.E.; Dixneuf, P.H.; Doucet, H.; Touzani, R.; Bellaoui, M. Identification of novel antifungal agents: Antimicrobial evaluation, SAR, ADME-Tox and molecular docking studies of a series of imidazole derivatives. *BMC Chem.* **2019**, *13*, 100. [CrossRef]

89. Biyiti, L.; Meko'o, D.; Tamzc, V.; Amvam Zollo, P. Recherche de l'activité antibactérienne de quatre plantes médicinales camerounaises. *Pharm. Med. Trad. Afr.* **2004**, *13*, 11–20.
90. Berche, P.; Gaillard, J.; Simonet, M. Les bactéries des infections humaines. Editeur: Flammarion. *Médecine Sci.* **1991**, 660. Available online: https://lib.ugent.be/en/catalog/rug01:000199668 (accessed on 17 February 2022).
91. Ennadir, J.; Hassikou, R.; Bouazza, F.; Arahou, M.; Al Askari, G.; Khedid, K. Évaluation in vitro de l'activité antibactérienne des extraits aqueux et organiques des graines de Nigella sativa L. et de Foeniculum vulgare Mill. *Phytothér* **2014**, *12*, 302–308. [CrossRef]
92. Bender, A.; Glen, R.C. Molecular similarity: A key technique in molecular informatics. *Org. Biomol. Chem.* **2004**, *2*, 3204–3218. [CrossRef] [PubMed]
93. Gleeson, M.P.; Hersey, A.; Montanari, D.; Overington, J. Probing the links between in vitro potency, ADMET and physicochemical parameters. *Nat. Rev. Drug Discov.* **2011**, *10*, 197–208. [CrossRef] [PubMed]
94. Fei, J.; Zhou, L.; Liu, T.; Tang, X.Y. Pharmacophore modeling, virtual screening, and molecular docking studies for discovery of novel Akt2 inhibitors. *Int. J. Med. Sci.* **2013**, *10*, 265–275. [CrossRef] [PubMed]
95. Skariyachan, S.; Pachiappan, A.; Joy, J.; Bhaduri, R.; Aier, I.; Vasist, K.S. Investigating the therapeutic potential of herbal leads against drug resistant *Listeria monocytogenes* by computational virtual screening and *in vitro* assays. *J. Biomol. Struct. Dyn.* **2015**, *33*, 2682–2694. [CrossRef]
96. Leelananda, S.P.; Lindert, S. Computational methods in drug discovery. *Beilstein J. Org. Chem.* **2016**, *12*, 2694–2718. [CrossRef]
97. Fares, M.; Said, M.A.; Alsherbiny, M.A.; Eladwy, R.A.; Almahli, H.; Abdel-Aziz, M.M.; Ghabbour, H.A.; Eldehna, W.M.; Abdel-Aziz, H.A. Synthesis, Biological Evaluation and Molecular Docking of Certain Sulfones as Potential Nonazole Antifungal Agents. *Molecules* **2016**, *21*, 114. [CrossRef]
98. Nastasă, C.; Vodnar, D.C.; Ionuț, I.; Stana, A.; Benedec, D.; Tamaian, R.; Oniga, O.; Tiperciuc, B. Antibacterial Evaluation and Virtual Screening of New Thiazolyl-Triazole Schiff Bases as Potential DNA-Gyrase Inhibitors. *Int. J. Mol. Sci.* **2018**, *19*, 222. [CrossRef]
99. Aggarwal, S.; Paliwal, D.; Kaushik, D.; Gupta, G.K.; Kumar, A. Pyrazole Schiff Base Hybrids as Anti-Malarial Agents: Synthesis, In Vitro Screening and Computational Study. *Comb. Chem. High Throughput Screen.* **2018**, *21*, 194–203. [CrossRef]
100. Hessler, G.; Baringhaus, K.H. Artificial Intelligence in Drug Design. *Molecules* **2018**, *23*, 2520. [CrossRef]
101. Muchtaridi, M.; Dermawan, D.; Yusuf, M. Molecular Docking, 3D Structure-Based Pharmacophore Modeling, and ADME Prediction of Alpha Mangostin and Its Derivatives against Estrogen Receptor Alpha. *J. Young-Pharm.* **2018**, *10*, 252–259. [CrossRef]
102. Holm, L. Benchmarking fold detection by DaliLite v.5. *Bioinformatics* **2019**, *35*, 5326–5327. [CrossRef] [PubMed]
103. Sangpheak, K.; Tabtimmai, L.; Seetaha, S.; Rungnim, C.; Chavasiri, W.; Wolschann, P.; Choowongkomon, K.; Riungrotmongkol, T. Biological Evaluation and Molecular Dynamics Simulation of Chalcone Derivatives as Epidermal Growth Factor-Tyrosine Kinase Inhibitors. *Molecules* **2019**, *24*, 1092. [CrossRef] [PubMed]
104. Sharma, D.; Kumar, S.; Narasimhan, B.; Ramasamy, K.; Lim, S.M.; Shah, S.A.A.; Mani, V. 4-(4-Bromophenyl)-thiazol-2-amine derivatives: Synthesis, biological activity and molecular docking study with ADME profile. *BMC Chem.* **2019**, *13*, 60. [CrossRef] [PubMed]
105. Curreli, F.; Ahmed, S.; Victor, S.M.B.; Ilusupov, I.R.; Belov, D.S.; Markov, P.O.; Kurkin, A.V.; Altieri, A.; Bebnath, A.K. Preclinical Optimization of gp120 Entry Antagonists as anti-HIV-1 Agents with Improved Cytotoxicity and ADME Properties through Rational Design, Synthesis, and Antiviral Evaluation. *J. Med. Chem.* **2020**, *63*, 1724–1749. [CrossRef]
106. Daina, A.; Michielin, O.; Zoete, V. SwissADME: A free web tool to evaluate pharmacokinetics, drug-likeness and medicinal chemistry friendliness of small molecules. *Sci. Rep.* **2017**, *7*, 42717. [CrossRef]
107. Abdellattif, M.H.; Abdel-Rahman, A.A.H.; Arief, M.M.H.; Mouneir, S.M.; Ali, A.; Hussien, M.A.; Okasha, R.M.; Afifi, T.H.; Hagar, M. Novel 2-Hydroselenonicotinonitriles and Selenopheno[2, 3-b]pyridines: Efficient Synthesis, Molecular Docking-DFT Modeling, and Antimicrobial Assessment. *Front. Chem.* **2021**, *9*, 672503. [CrossRef]
108. Drwal, M.N.; Banerjee, P.; Dunkel, M.; Wettig, M.R.; Preissner, R. ProTox: A web server for the in silico prediction of rodent oral toxicity. *Nucleic Acids Res.* **2014**, *42*, W53–W58. [CrossRef]
109. Shehab, W.S.; Abdellattif, M.H.; Mouneir, S.M. Heterocyclization of polarized system: Synthesis, antioxidant and anti-inflammatory 4-(pyridin-3-yl)-6-(thiophen-2-yl) pyrimidine-2-thiol derivatives. *Chem. Cent. J.* **2018**, *12*, 68. [CrossRef]
110. Yeni, S.; Merdekawati, F. In Silico Study of Pyrazolylaminoquinazoline Toxicity by Lazar, Protox, and Admet Predictor. *J. Appl. Pharm. Sci.* **2018**, *8*, 119–129.
111. Abdellattif, M.H.; Shahbaaz, M.; Arief, M.M.H.; Hussien, M.A. Oxazinethione Derivatives as a Precursor to Pyrazolone and Pyrimidine Derivatives: Synthesis, Biological Activities, Molecular Modeling, ADME, and Molecular Dynamics Studies. *Molecules* **2021**, *26*, 5482. [CrossRef] [PubMed]
112. Banerjee, P.; Eckert, A.O.; Schrey, A.K.; Preissner, R. ProTox-II: A webserver for the prediction of toxicity of chemicals. *Nucleic Acids Res.* **2018**, *46*, 257–263. [CrossRef] [PubMed]
113. Ramos, R.D.S.; Costa, J.D.S.; Silva, R.C.; da Costa, G.V.; Rodrigues, A.B.L.; Rabelo, E.D.M.; Souto, R.N.P.; Taft, C.A.; Silva, C.H.T.D.P.D.; Rosa, J.M.C.; et al. Identification of Potential Inhibitors from Pyriproxyfen with Insecticidal Activity by Virtual Screening. *Pharmaceuticals* **2019**, *12*, 20. [CrossRef] [PubMed]
114. Frisch, M.J.; Trucks, G.W.; Schlegel, H.B.; Scuseria, G.E.; Robb, M.A.; Cheeseman, J.R.; Scalmani, G.; Barone, V.; Petersson, G.A.; Nakatsuji, H.; et al. *Gaussian 09, Revision A.02*; Gaussian, Inc.: Wallingford, CT, USA, 2016.

115. Rizvi, S.M.D.; Shakil, S.; Haneef, M. A simple click by click protocol to perform docking: Autodock 4.2 made easy for non-bioinformaticians. *EXCLI J.* **2013**, *12*, 831–857. [PubMed]
116. Vieira, T.F.; Sousa, S.F. Comparing AutoDock and Vina in Ligand/Decoy Discrimination for Virtual Screening. *Appl. Sci.* **2019**, *9*, 4538. [CrossRef]
117. Kaddouri, Y.; Abrigach, F.; Ouahhoud, S.; Benabbes, R.; El Kodadi, M.; Alsalme, A.; Al-Zaqri, N.; Warad, I.; Touzani, R. Mono-Alkylated Ligands Based on Pyrazole and Triazole Derivatives Tested Against Fusarium oxysporum f. sp. albedinis: Synthesis, Characterization, DFT, and Phytase Binding Site Identification Using Blind Docking/Virtual Screening for Potent Fophy Inhibitors. *Front. Chem.* **2020**, *8*, 559262.
118. Hall, C.; Nelson, D.M.; Ye, X.; Baker, K.; DeCaprio, J.A.; Seeholzer, S.; Lipinski, M.; Adams, P.D. Hira, the human homologue of yeast hir1p and hir2p, is a novel cycin-cdk2 substrate whose expresssion blocks S-phase progresssion. *Mol. Cel. Biol.* **2001**, *21*, 1854–1865. [CrossRef]
119. DeGoey, D.A.; Chen, H.J.; Cox, P.B.; Wendt, M.D. Beyond the Rule of 5: Lessons Learned from AbbVie's Drugs and Compound Collection. *J. Med. Chem.* **2018**, *61*, 2636–2651. [CrossRef]
120. Caron, G.; Digiesi, V.; Solaro, S.; Ermondi, G. Flexibility in early drug discovery: Focus on the beyond-Rule-of-5 chemical space. *Drug Discov. Today* **2020**, *25*, 621–627. [CrossRef]